A Multidimensional Gas Chromatographic Method for Analysis of *n*-Butane Oxidation Reaction Products

P.L. Mills*

DuPont Company, Experimental Station, E262/100D, Chemical Science and Engineering Laboratory, Wilmington, DE 19880-0262

W.E. Guise, Jr.

Argonne National Laboratory, Advanced Photon Source, 9700 S. Cass Ave., Argonne, IL 60639

Abstract

A multidimensional gas chromatographic (GC) method for on-line analysis of all gas-phase reaction products obtained from the selective oxidation of *n*-butane to maleic anhydride in an automated catalyst testing reactor is described.

A dimethylpolysiloxane megabore column and a multidimensional sequence of packed columns that contain molecular sieve 5A and Hayesep R are shown to provide resolution of *n*-butane, maleic anhydride, various oxygen-containing byproducts, oxygen, nitrogen, and all total combustion products by using a single temperature programmed GC with simultaneous injection of two gas samples from a multiport valve. For applications where various C_1–C_4 hydrocarbon byproducts are either known or suspected to be present in the product gas and precise resolution is required, an Al_2O_3/KCl PLOT column can be connected to the dimethylpolysiloxane column by using a series-bypass arrangement with a multiport valve. All hydrocarbons and oxygen-containing hydrocarbons are detected with a flame-ionization detector, and a thermal conductivity detector is used for the permanent gases, total combustion products, and *n*-butane. To quantify the raw GC peak areas, both absolute and relative response factors are also derived for all species by using gas-phase and liquid-phase calibration standards. Comparisons between experimental and theoretical values for the relative effective carbon numbers of maleic anhydride with those of *n*-butane are also used to confirm that solute adsorption is linear and reversible on the selected megabore column. Effective carbon numbers for the other analytes detected by the flame-ionization detector are also derived and compared with the theoretical values. Statistical characterization of the response factors and effective carbon numbers is also performed so that an assessment of the errors associated with any derived quantities in future applications of the method, such as gas compositions, reactant conversions, and product yields, will be possible. Incorporation of the proposed method into an automated fixed-bed catalyst test facility and typical results obtained for *n*-butane oxidation to maleic anhydride over a known metal oxide catalyst are also described. Advantages of the proposed technique over previously reported GC methods for analysis of the reaction products from butane oxidation are also suggested.

* Author to whom correspondence should be addressed.

Introduction

Maleic anhydride is an important chemical intermediate that is manufactured by the vapor-phase selective oxidation of benzene, butylenes, or *n*-butane over heterogeneous metal-oxide catalysts by using fixed-bed or fluidized-bed reactors (1–6). Butane is the preferred hydrocarbon feedstock in most modern processes due to its lower cost, greater availability, and lower toxicity when compared with either benzene or butylenes (7,8). Various aspects of catalyst performance evaluation, such as screening of new or improved catalyst compositions, determination of reaction pathways, discrimination between rival reaction kinetic models, evaluation of long-term catalyst performance, and catalyst optimization, are often performed in laboratory or pilot-scale reactor systems (9). An analytical system that can resolve and quantitate the primary and secondary reaction products over a range of reaction conditions is essential for interpretation of overall reactor performance and for evaluation of catalyst performance parameters (10). Implementation of the analytical system as a direct, on-line technique is also desirable, since data acquisition of both the reactor process variables and gas-phase species compositions can then be controlled and processed by a computer at predetermined time intervals with precision and accuracy. Use of one or more analytical systems in series or parallel to monitor multiple reactor systems for short or extended periods of operation also becomes a reality. This is particularly useful during exploratory phases of catalyst testing, since the discovery process involves preparation and performance evaluation of many catalyst compositions (11).

Exploratory catalyst research on *n*-butane oxidation poses a significant challenge for an automated analytical system because of the variety of reaction pathways that can exist. Maleic anhydride, various partial oxidation byproducts, C_2–C_4 hydrocarbons, carbon oxides, and water can be produced during the execution of a typical catalyst evaluation test protocol that uses reaction temperature, total pressure, gas feed composition, and feed flow rate or contact time as experimental parameters (12,13). Unless the nature of the reaction products can be determined or speculated beforehand, some caution must be

Table I. Indirect Methods for Analysis of Maleic Anhydride in Gas-Phase Catalyzed Oxidations and Ammoxidations
(continued on Page 433)

Application	Species	Columns	Reference
cis-Butene-2 oxidation	Organic products, including maleic anhydride	15% PEG 4000 on firebrick	41
Methylcyclopentane oxidation	Dimethyl maleate; dimethyl citraconate; maleic anhydride; citraconic anhydride	25% di-2-ethyl hexyl sebacate + 10% sebacic acid on Chromosorb P AW	42
Naphthalene oxidation	Maleic anhydride; naphthalene; benzyl alcohol; 1,4-naphthoquinone	10% PFMS-6 silicon oil on 3:1 Chromosorb W	43
Naphthalene oxidation	Maleic anhydride; naphthalene; benzoic acid; phthalic anhydride; 1,4-naphthoquinone	10% PFMS-6 silicon oil on 3:1 Chromosorb W-TND-TSM	44
Naphthalene and *ortho*-xylene oxidation	Oxygen; nitrogen; carbon monoxide;	Molecular Sieve 13X	45
	Carbon dioxide	Porapak Q	
	Maleic anhydride; phthalaldehyde; benzene; *ortho*-tolualdehyde; benzyl alcohol; 4-methylphthalic acid; phthalide; phthalimide; naphthalene; *ortho*-xylene	DC-200 silicone oil on Chromosorb W (after adsorption of products in acetone)	
Naphthalene oxidation	Maleic anhydride; naphthalene; benzoic acid; phthalic anhydride; α-naphthoquinone; phthalimide	Apiezon M (using crude phthalic anhydride)	46
Naphthalene oxidation	Carbon dioxide and carbon monoxide	Activated carbon and NaX Zeolites	47
	Maleic anhydride; phthalic anhydride; naphthalene; 1,4-naphthoquinone	25% E-301 polymethylsiloxane on Chromosorb W (after absorption of products in *o*-xylene)	
ortho-Xylene oxidation	Maleic anhydride; phthalic anhydride; phthalide; *o*-toluic aldehyde; *o*-xylene	1% H_3PO_4 + 5% PFMS-4 silicone oil on Chromosorb A (after absorption of products in propylene carbonate)	48
ortho-Xylene oxidation	Maleic anhydride; phthalic anhydride; phthalide; *o*-toluic acid; *o*-tolualdehyde	OV-225 on graphitized thermal carbon black	49

exercised to ensure that the resolution and quantification of the primary reactants and products—in other words, *n*-butane, oxygen, maleic anhydride, carbon oxides, and water—are not corrupted by the presence of one or more unidentified species. Reaction intermediates and side-products that have been reported in the literature when either *n*-butane or various butylenes are used as the carbon source include butenes, butadiene, crotonaldehyde, dihydrofuran, furan, crotonic acid, acrylic acid, methacrylic acid, acetic acid, acetone, acetaldehyde, formaldehyde, glyoxylic acid, methyl ethyl ketone, methyl vinyl ketone, carbon oxides, and water (14–29). Although reaction pathways that describe the formation of these species from *n*-butane or butylenes have been suggested (12,27), detailed reaction studies that quantitate the various extents of reaction for each pathway for a well-characterized catalyst have not been reported to our knowledge.

Routine performance evaluations of commercial catalyst samples for *n*-butane oxidation generally yield reaction product mixtures that contain fewer byproducts than those encountered during exploratory catalyst research (23,30). In this particular type of application, the reaction conditions and catalyst compositions have been previously identified so that the net formation of byproducts is minimized relative to the formation of maleic anhydride. Several recent kinetic studies on *n*-butane oxidation in fixed-bed microreactors where the oxygen concentration is maintained at a stoichiometric excess have shown that carbon oxides and water are the only byproducts (31–38). Some other investigators indicated that the formation of ethylene, butenes, butadiene, acetaldehyde, acrolein, acetic acid, and acrylic acid can be detected when the concentration of gas-phase oxygen approaches 0 at or before the reactor exit that corresponds to a stoichiometric excess of *n*-butane in the feed gas (25,26,39). Resolution of the C_2–C_4 hydrocarbons and C_1–C_2 aldehydes and acids, in addition to maleic anhydride, would be necessary under these reaction conditions. Attention to these subtle, but important, details are often omitted or very lightly sketched in the cited applications.

Literature review

Various methods (e.g., infrared spectroscopy, nuclear magnetic resonance, polarographic reduction, titrimetric methods, and chromatographic analysis [1,2]) have been developed for

Table I. Indirect Methods for Analysis of Maleic Anhydride in Gas-Phase Catalyzed Oxidations and Ammoxidations ***(continued from Page 432)***

Application	Species	Columns	Reference
ortho-Xylene and naphthalene oxidation and ammoxidation	Organic oxidation and ammoxidation reaction products	15% DC-550 silicone oil on Chromaton N-AW with DMCS	50
Toluene oxidation	Benzaldehyde; phenol; cresols; benzoic acid; maleic anhydride; anthraquinone	5% OV-101 on Chromosorb G HP (100–120 mesh)	51
Maleic anhydride hydrogenation	Diethyl maleate; diethyl succinate; γ-butyrolactone; tetrahydrofuran; 1,3- and 1,4-butanediol; 2-pyrrolidine	3% PEG Adipate on Chromaton NAW DMCS	52
	Maleic anhydride; succinic anhydride; 1-butanol; 1-propanol; tetrahydrofuran	10% SE-30 on Chromaton NAW DMCS	
Maleic anhydride hydrogenation	γ-Butyrolactone; tetrahydrofuran; succinic anhydride; propionic acid; butyric acid; 1-propanol; 1-butanol; maleic anhydride	3% Neopentyl Glycol Succinate with 1% H_4PO_4	53
Maleic anhydride hydrogenation	Maleic acid; maleic anhydride; acetic acid; propionic acid; isobutyric acid	5% GE-XF-1150 silicone oil on Fluoropak 80	54
Maleic anhydride hydrogenation	*n*-Butyric acid; γ-butyrolactone; maleic anhydride; succinic anhydride; succinic acid	2.7% XE on Chromosorb G AW (DMF internal standard) 20% DC-550 silicone oil on Chromosorb W (Et phenyl acetate internal standard)	55
Maleic acid hydrogenation	γ-Butyrolactone; maleic anhydride; succinic anhydride; *N*-methylsuccinimide; *N*-methyl-2-pyrrolidine; tetrahydrofuran; water	Chromosorb 102	56
Air quality assessment	Organic contaminants, including maleic anhydride	Tenax GC	57, 58
Groundwater solid waste quality assessment	> 270 species, including maleic anhydride	Supercritical fluid chromatography	59, 60
Polymer impurities	Propylene oxide; epichlorohydrin; maleic anhydride; propylene glycol; and other impurities	Porapak Q	61

quantitative analysis of maleic anhydride in applications that range from its manufacture to various end uses. Although each of these methods has advantages and disadvantages, gas chromatography (GC) is particularly well-suited for gas-phase catalytic reactor applications from the perspective of sample handling and introduction, sample resolution, analysis time, qualitative analysis, and quantitative analysis. For these reasons and several others that are omitted for brevity, various methods based on gas and gas–liquid chromatography have been developed to analyze the reaction products from the catalytic partial oxidation of butane or butylenes to maleic anhydride and the corresponding byproducts. These can be broadly classified as being either direct or indirect methods, which are differentiated according to whether the reaction product gas is subjected to some type of pretreatment before analysis. Development of chromatographic techniques that use either method are generally complicated by gas sample handling problems due to the high melting point (52.8°C) and elevated boiling point (202°C at 1 atm) of maleic anhydride (2). Another complication is the identification of a chromatographic packing or stationary phase with which the adsorption of maleic anhydride and other oxygen-containing reaction byproducts is linear and reversible but which provides the necessary species resolution. The use of the effective carbon number concept to properly evaluate GC columns for analysis of maleic anhydride and other potentially reactive solutes has been presented (40) but has not been widely used.

The implementation of indirect methods for analysis of maleic anhydride from C_4 hydrocarbon oxidations and other catalytic reactions has been performed with several approaches. A summary of the applications, species analyzed and quantitated, and columns used is given in Table I. The differences that exist are mainly in the methodology and GC column used to isolate maleic anhydride and other oxygenated hydrocarbons. In one approach (29,35–39), the reactor product gas is continuously bubbled into a cooled water trap to condense maleic anhydride and any other water-soluble products. The resulting off-gas is then passed through a condenser that is maintained at a slightly higher temperature than the trap. It is then analyzed for the permanent gases, carbon monoxide, carbon dioxide, and noncondensable hydrocarbons by using a sequence of packed columns that contain Porapak Q and molecular sieve 5A with the thermal conductivity detector (TCD). The maleic

Table II. Direct Methods for Analysis of Maleic Anhydride in Gas-Phase Catalyzed Oxidations

Application	Species	Columns	Reference
n-Butane oxidation	Oxygen; nitrogen; carbon monoxide	Molecular Sieve 13X	31
	Carbon dioxide	20% bis (2-methoxyethyl) adipate on Chromosorb P AW	
	C_1–C_4 hydrocarbons (maleic anhydride was not analyzed)	Chromosorb P AW	
n-Butane oxidation	Oxygen; nitrogen; carbon monoxide	Molecular Sieve	32
	Carbon dioxide	Porapak N (80–100 mesh)	
	C_4 hydrocarbons	EES P (60–80 mesh)	
	Organic products, including maleic anhydride	Porapak QS	
n-Butane oxidation	Oxygen; nitrogen; carbon monoxide	Molecular Sieve	39
	Ethylene; *n*-butane; acrolein; acetic acid; acrylic acid; maleic anhydride	Porapak QS	
n-Butane oxidation	Organic products, including maleic anhydride	AT-1000 fused silica; DEGS stainless steel SCOT; Glass OV-1	40
n-Butene-1 oxidation	Carbon monoxide	Molecular Sieve 13X (100–120 mesh, 1 m x 3-mm i.d.)	63
	Carbon dioxide; *n*-butene-1; *trans*-butene-2; *cis*-butene-2; butadiene	Dimethylsulpholane on Chromosorb (30–80 mesh, 5 m x 3-mm i.d.)	
	C_4 hydrocarbons; furan; isobutyraldehyde; α-Me-acrylaldehyde; butanone; crotonaldehyde; acetic acid; propionic acid; acrylic acid; maleic anhydride	Di (2-ethylhexyl) sebacate + sebacic acid on Chromosorb P AW (2 m x 2-mm i.d.)	
n-Butene-1 oxidation	*n*-Butene-1; *cis* + *trans*-Butene-2; butadine	Porapak R	64
	C_4 hydrocarbons; acetaldehyde; crotonaldehyde; propionaldehyde; maleic anhydride	SE-30 silicone oil or di-isodecylphthalate on Chromosorb P AW-DMCS	
n-Butane oxidation	Acetaldehyde; acetone; acrolein; methacrolein; acetic acid; acrylic acid; maleic anhydride	Glass column, 100 cm (packing not specified)	65, 66
n-Butane oxidation	Oxygen; nitrogen; carbon monoxide	Molecular Sieve at 80°C	67
	Carbon dioxide; ethylene, water; propane; formaldehyde; acetaldehyde; isobutane; *n*-butane	Porapak Q at 80°C	
	C_4 hydrocarbons; acetone, acrolein, propionaldehyde (composite peak); acetic acid; methyl vinyl ketone; methyl ethyl ketone; crotonaldehyde; butanedione; maleic anhydride	Porapak Q at 150°C	
n-Butane oxidation	Carbon monoxide; Carbon dioxide; hydrogen	Carbosieve B (TCD)	68
	Hydrocarbons	Porasil C (FID)	
	Hydrocarbons and oxygenates	Porapak Q (FID)	
o-Xylene oxidation	Nitrogen; carbon monoxide; carbon dioxide	Molecular Sieve 5A	69
	Hydrocarbons and oxygenates	Porapak Q and 10% SE-52 on Chromosorb W	
o-Xylene oxidation	*o*-Xylene reaction products	SE-30	70
Benezene oxidation	Oxygen; nitrogen; carbon monoxide	Molecular Sieve 5A	71
	Carbon dioxide;	Porapak Q at 50°C	
	Benezene; maleic anhydride	Porapak Q at 185°C or 20% SE-96 on Chromosorb W	
Toluene oxidation	Carbon monoxide; carbon dioxide	Chromosorb 102	72
	Toluene; benzaldehyde	5% OV-101 on Chromosorb G	

anhydride and any other condensed species are analyzed off-line by manual injections by using another Porapack Q column connected to a flame-ionization detector (FID). Since maleic anhydride dissolves in water with simultaneous hydrolysis to yield maleic acid (1,2), it is actually the latter species that is being detected on the FID. To verify the chromatographic results, titration of the maleic acid against an aqueous base, such and NaOH or KOH, to the two end points at pH 3.7 and 9.5, respectively, is sometimes used (2). A variation of this technique used in the catalytic oxidation of *o*-xylene or naphthalene to phthalic anhydride employs a nonreacting organic solvent instead of water, such as acetone (45,46), *o*-xylene (47), or propylene carbonate (48), to trap the maleic anhydride and other soluble reaction products without conversion to the corresponding acids. Analysis of this mixture and the noncondensable species uses the same or a similar system of packed columns. The use of acetone would also permit the independent determination of acid impurities by potentiometric titration with a standard solution of tripropylamine or *N*-ethylpiperidine (2). Derivatization of maleic anhydride to dimethylmaleate with an H_2SO_4–MeOH mixture before conducting the chromatographic analysis has also been reported (42). Applications where quantitative analysis of the water vapor in the reactor effluent is needed could not use this approach, since the actual water concentration would be altered by the various postreactor bubblers, traps, and condensers. One reaction kinetics study showed that the addition of excess water vapor has a net positive effect on maleic anhydride selectivity and an inhibiting effect on the observed reaction rate (39), and another study shows that it has a negligible effect (62) (J.B. Benziger, S. Sundaresan, and V.V. Guliants, unpublished data).

Direct methods for analysis of the reaction product gases produced from the catalytic oxidation of *n*-butane or butylenes differ from indirect methods because the reaction sample is ideally not subjected to pretreatment before injection. The sample is obtained from a gas-sampling valve and injected directly so that manual handling of a condensed aqueous or organic liquid phase is avoided. Appropriate hardware and measures are needed to collect the live reaction sample without sublimation or thermal decomposition of the maleic anhydride from the vapor-phase mixture. Direct methods may also involve the use of traps and condensers to prevent high boiling species from irreversibly adsorbing on the columns used to analyze the lighter fraction of the reaction product gas (63). However, this introduces another degree of complexity in the system operation.

Table II shows a summary of various applications in gas-phase catalytic oxidations in which direct methods for on-line analysis have been used to resolve and quantitate the reaction product gases. This is not intended to be a comprehensive literature survey but is representative of various methods that are currently used. Maleic anhydride was the primary product when either *n*-butene-1, *n*-butane, or benzene served as the hydrocarbon source. In the remaining applications, such as the selective oxidation of either *o*-xylene or naphthalene to phthalic anhydride and toluene to benzaldehyde, maleic anhydride is an undesired reaction byproduct. These reactions are always accompanied by the formation of various byproducts that are also listed and presumably analyzed by the indicated method.

Analysis of maleic anhydride in the reaction products has relied mainly on the use of porous polymer packings, such as Porapak QS (32,39) and Porapak Q (67). Other methods have been developed that use one or more stationary phases on a solid support, such as di(2-ethylhexyl)sebacate + sebacic acid on Chromosorb W (63), silicone oils SE-30 (64), SE-52 (69), or SE-96 (71) all on Chromosorb W, and OV-101 on Chromosorb G (72). In one case (40), several different types of capillary columns, such as AT-1000 fused silica, a DEGS stainless steel SCOT, and a glass OV-1, were shown to exhibit the correct responses for maleic anhydride when comparisons were made between the experimental and theoretical relative effective carbon numbers. The incorporation of one of these capillary columns in a method that gives a complete analysis of all C_4 hydrocarbon oxidation products was not described. In addition, to

Table III. Columns Evaluated for Analysis of C_1–C_4 Hydrocarbons and Oxygenates

Column	Column Type	Column Dimensions		
		Diameter	Length	Film Thickness or Particle Size
Chrompack PLOT Al_2O_3/KCl	Megabore	0.53 mm	25 m	10.0 µm
Supelco 23% SP-1700 on Chromosorb P AW	Packed	1/8 in.	30 ft	80/100 mesh
J&W DB-1	Megabore	0.53 mm	30 m	1.5 µm
J&W DB-1	Megabore	0.53 mm	30 m	5.0 µm
J&W DB-5	Megabore	0.53 mm	30 m	1.5 µm
J&W DB-17	Megabore	0.53 mm	30 m	1.0 µm
J&W DB-210	Megabore	0.53 mm	30 m	1.0 µm
Restek 1701	Megabore	0.53 mm	30 m	3.0 µm
J&W DB-FFAP	Megabore	0.53 mm	30 m	1.0 µm
Supelco Nukol	Capillary	0.32 mm	30 m	1.0 µm
Chrompack PoraPLOT Q	Megabore	0.53 mm	25 m	NA*
Chrompack PoraPLOT U	Megabore	0.53 mm	25 m	NA*

*NA = not applicable.

our knowledge, none of the methods described in the literature provide a means of resolving and quantitating all of the species that are present in the partial oxidation of C_4 hydrocarbons to maleic anhydride, including water, by using a GC system that is equipped with both thermal conductivity and flame-ionization detectors. The ability to resolve and quantitate water cannot be underestimated, since several recent kinetic studies have shown that both the intrinsic reaction rates and selectivity or yield to maleic anhydride are affected by the concentration of this species in the reaction environment (39,62)(J.B. Benziger, S. Sundaresan, and V.V. Guliants, unpublished data). Therefore, the ability to quantitate the steam concentration in both the feed and product gas by a direct method versus through inference using the measured compositions of CO and CO_2 would be particularly useful.

Objectives

The primary objective of this study was to describe a direct method for on-line analysis of the product gas obtained from the partial oxidation of *n*-butane to maleic anhydride over metal oxide catalysts. The method described here is primarily intended for catalyst evaluation and catalytic reaction engineering applications where resolution of the product gas into the primary and secondary products and the precise quantitation of these products is required. Some particular applications where these results are expected to be useful include (*a*) performance evaluation and ranking of various proposed catalyst compositions; (*b*) catalyst quality control with use of one or more standardized catalyst testing protocols; (*c*) determination of reaction networks and reaction pathways; (*d*) discrimination between reaction mechanisms and reaction kinetic parameter estimation; and (*e*) monitoring of laboratory-scale, pilot-plant, and commercial-scale reactor performance. Although the emphasis here is placed on analysis of mixtures from catalytic reactions, it is expected that the proposed technique could be used, after minor modifications for sample introduction, to other application areas where the same or similar types of species are encountered. In addition to providing important details about the method, this study also illustrates a typical application from a typical catalyst evaluation experiment by using an automated butane oxidation catalyst testing system.

Table IV. Columns Evaluated for Analysis of Oxygen, Nitrogen, Carbon Oxides, Water, and *n*-Butane

Column	Column Type	Column Dimensions: Diameter (in.)	Length (ft)	Film Thickness or Particle Size
Supelco Hayesep A	Packed	1/8	3	100/120 mesh
Supelco Hayesep D	Packed	1/8	4	80/100 mesh
Supelco Hayesep Q	Packed	1/8	6	80/100 mesh
Supelco Hayesep R	Packed	1/8	2	80/100 mesh
Supelco Hayesep R	Packed	1/8	6	80/100 mesh
Supelco Hayesep T	Packed	1/8	5	80/100 mesh
Chromosorb 102	Packed	1/8	6	80/100 mesh
Porapak QS	Packed	1/8	6	80/100 mesh
Molecular Sieve 5A*	Packed	1/8	6	60/80 mesh
Molecular Sieve 5A	Packed	1/8	12	60/80 mesh
Molecular Sieve 5A	Packed	1/8	13	60/80 mesh
Molecular Sieve 5A	Packed	1/8	14	60/80 mesh
Molecular Sieve 5A	Packed	1/4	6	60/80 mesh
Molecular Sieve 5A	Packed	1/4	14	60/80 mesh

*This column was also evaluated using an argon carrier gas.

Table V. Gas and Liquid Calibration Standards

Compound	mol%	Compound	wt%	Compound	mol%
Methane	1.030	Formaldehyde	3.537	Nitrogen	75.105
Acetylene	1.080	Acetone	80.665	Oxygen	19.965
Ethane	1.090	Furan	1.697	Carbon monoxide	0.970
Ethylene	1.090	Methacrolein	1.093	Carbon dioxide	1.030
Propane	0.992	2,3-Dihydrofuran	1.198	Argon	2.930
Propylene	1.030	MEK	1.112		
n-Butane	1.010	Glyoxylic acid	2.128		
iso-Butane	3.970	Acetic acid	1.093		
1-Butene	1.010	Tetrahydrofuran	1.102		
trans-2-Butene	0.995	Crotonaldehyde	0.959		
cis-2-Butene	1.080	Acrylic acid	1.064		
iso-Butylene	4.010	Isobutyric acid	1.016		
1,3-Butadiene	0.991	Methacrylic acid	1.332		
Nitrogen	81.632	Maleic anhydride	1.045		
		Crotonic acid	0.959		
Total	100		100		100

Experimental

Equipment

All analyses were performed by using a Hewlett-Packard Model 5890 Series II gas chromatograph (Palo Alto, CA) equipped with both an FID and a TCD. The FID side was used for analysis of hydrocarbons and oxygenates with capillary columns operated in the split mode (40:1); it was equipped with a split/splitless capillary injector. The TCD side was used for analysis of permanent gases (e.g., oxygen and nitrogen), carbon dioxide, carbon monoxide, water, and unreacted *n*-butane with packed columns; it contained a purged/packed column injector inlet. Helium was used as the column carrier gas for both the capillary and packed columns at volumetric flow rates of 10 and 60 cm^3/min, respectively. Make-up gas was not added before the FID because the capillary column flow rates were adequate. The hydrogen and air flow rates to the FID were set at 30 and 450 cm^3/min, respectively, as specified by the manufacturer. The helium flow rate on the reference side of the TCD was set at 90 cm^3/min. Temperatures for both injectors and detectors were set at 230°C and 250°C, respectively. The FID electrometer sensitivity was usually set at a range of 3 and at an attenuation of 4. The TCD was operated at the high sensitivity setting with a range of unity.

The analog output signals for both detectors were connected to separate channels of a VG four-channel chromatography data server (Part No. MX-CS400) that was connected to a DEC VAX Model 6510 computer for subsequent signal processing, graphical display on a CRT, and storage on a hard disc using VG Multichrom Version 5.5-1. The output signals for either detector were also connected to a Hewlett-Packard Model 3396 Integrator and used for local display on chart paper. The chromatograms that are illustrated in the Results and Discussion section are direct reproductions produced from the latter device.

These two configurations were used to acquire the data for off-line operation during method development and for on-line operation corresponding to direct analysis of the reactor product gases by using a sampling valve. Typical method development activities included initial column screening, evaluation of peak resolution and relative response times, determination of column efficiencies, and assessment of absolute and relative response factors.

Since the ultimate application of the method was on-line analysis of butane oxidation reaction products from a catalytic reactor system, the inlet tubing to each injector was modified to permit either a manual syringe injection for the various method development activities listed above or on-line injection from a 10-port Valco gas-sampling valve. The sampling valve was configured with two 500-µL sample loops so that the same gas sample could be collected and injected to the specific columns associated with a given detector. The sample transfer line

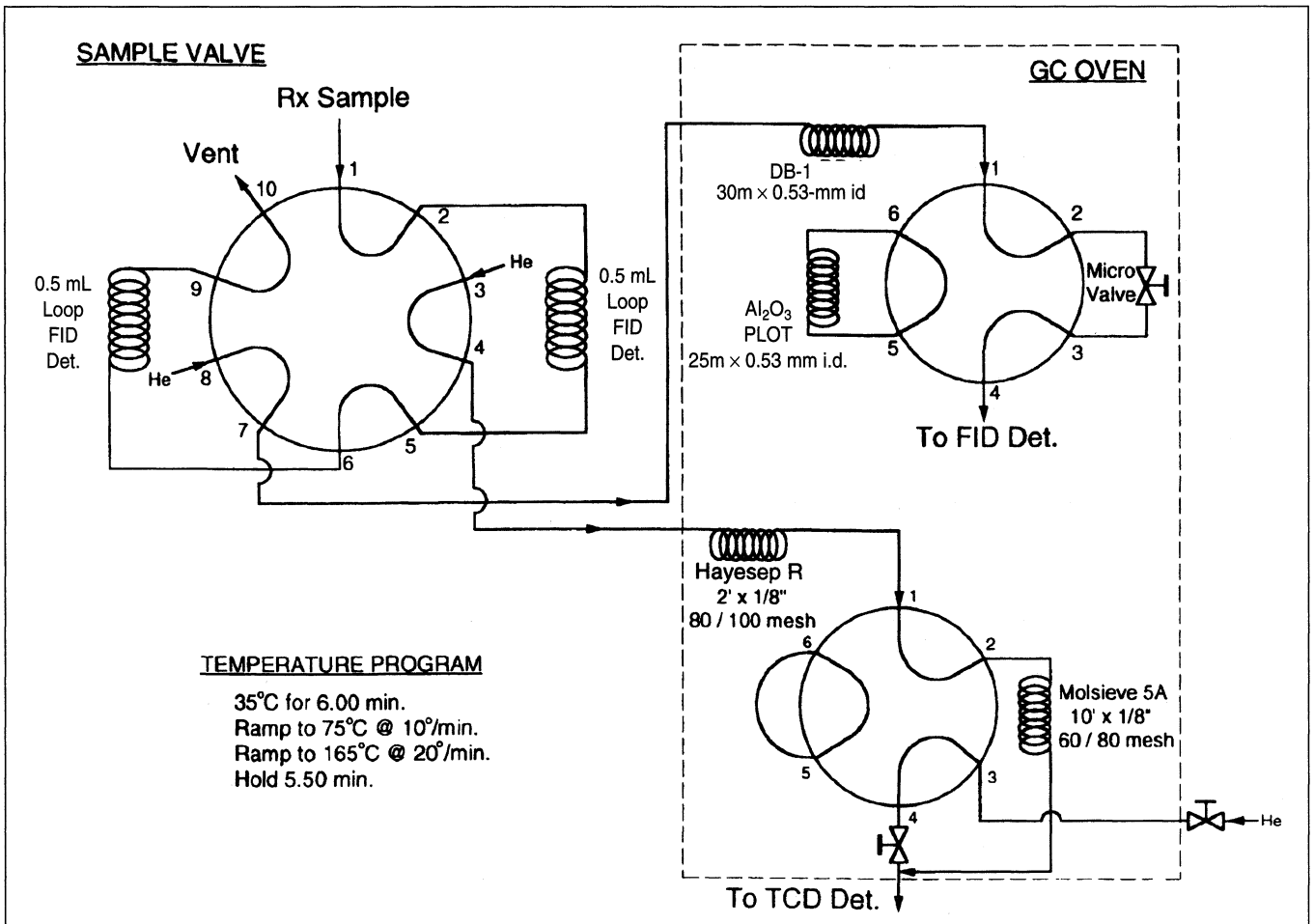

Figure 1. Flow diagram of the final method. Solid lines indicate valve position 1 (off), and dashed lines indicate valve position 2 (on).

between the valve oven and the GC injector was $\frac{1}{16}$-in. o.d. stainless steel tubing with a fused silica lining (Silicosteel; Restek, Bellefonte, PA) to eliminate or minimize sample adsorption. The deactivation layer is absent to permit operation up to 600°C.

Response factors for selected nonvolatile species, such as maleic anhydride, water, and tetrahydrofuran, were also determined by using the on-line sampling valve for comparison with those derived from manual injection. This was performed by continuously pumping a binary liquid solution containing 1 wt% water in acetone or a ternary liquid solution containing 1 wt% maleic anhydride and 1 wt% tetrahydrofuran in acetone to a special-purpose in-line mixer–vaporizer with a precision HPLC pump (Model LC-5000; ISCO, Lincoln, NE). The vaporizer was designed to generate small liquid droplets that were contacted with a flowing nitrogen stream in a mixing zone from which a homogeneous, superheated vapor was produced. The mixer–vaporizer was normally used to generate steam for addition to the reactor feed gas for certain catalyst testing experiments. The resulting mixture was periodically sampled on-line and analyzed by using the method described below. All other calibration experiments involving gas mixtures were performed by direct on-line sampling of the flowing mixture through one of the mass flow controller loops in the reactor feed system manifold.

Columns

A variety of capillary and packed columns with a wide range of polarities were evaluated during the initial part of this effort for resolution of liquid and gas test mixtures where the species and compositions in these mixtures were either speculated or based on those given in the literature (13–39). A summary of the columns and their specifications is given in Tables III and IV. The columns were used as received from the commercial supplier; they were conditioned following the recommendation of the manufacturer before conducting any test evaluations.

The capillary columns were intended for analysis of the C_1–C_4 hydrocarbons as well as various oxygen-containing organic compounds produced from *n*-butane oxidation by using the FID. The packed columns were selected with the intention of finding a suitable combination capable of resolving the permanent gases, carbon monoxide, carbon dioxide, water, *n*-butane, and a noble gas with the TCD. The latter component was sometimes added to the feed gas as an internal standard for certain types of reaction experiments at concentrations of 1–5 mol%. This concentration range was close to the expected magnitude for the major reaction products, such as butane, maleic anhydride, the carbon oxides, and water. Nitrogen was present in the reactor feed gas and could be used as an internal standard, but the concentration was typically 72–77 mol%, which was between 1 and 2 orders of magnitude greater than that of these products. This large difference in concentration proved to be a source of error when material balance calculations were performed with the internal standard method for quantitation, since the area and concentration ratios produced quotients derived from the ratio of nu-

Table VI. Time versus Event Schedule for the Valve Sequencing for Samples that Contained a Simpler Hydrocarbon Matrix

Elapsed Time (min)	Flow Valve	Sample Valve	Valve 1 (FID)	Value 2 (TCD)	Event
< 0	1	1	1	1	Preinjection condition
0.0	0	1	1	1	Direct reactor off-gas to fill sample loops.
2.0	1	1	1	1	Sample loops filled; initiate sample loop depressurization
2.3	1	0	1	1	Complete sample loop depressurization and inject samples
3.2	1	0	1	0	Switch from series flow path to parallel column flow path on the TCD side
4.0	1	1	1	0	Ready sample valve for the next sample
17.9	1	1	1	1	Switch from parallel column flow path to series column flow path on the TCD side

Table VII. Time versus Event Schedule for the Valve Sequencing for Samples that Contained a More Complex C_1–C_4 Hydrocarbon Matrix

Elapsed Time (min)	Flow Valve	Sample Valve	Valve 1 (FID)	Value 2 (TCD)	Event
< 0	1	1	0	1	Preinjection condition
0.0	0	1	0	1	Direct reactor off-gas to fill sample loops
2.0	1	1	0	1	Sample loops filled; initiate sample loop depressurization
2.3	1	0	0	1	Complete sample loop depressurization and inject samples
4.2	1	0	1	1	Hydrocarbons trapped on Al_2O_3/KCl PLOT column; elute oxygenates from DB-1 column
5.1	1	0	1	0	Switch from series flow path to parallel column flow path on the FID side
6.0	1	1	1	0	Ready sample valve for next sample
17.9	1	1	1	1	Switch from parallel column flow path to series column flow path on TCD side
18.0	1	1	0	1	Bring Al_2O_3/KCl PLOT column back on-line and elute hydrocarbons, including return to preinjection condition

merators and denominators that varied by at least 2 orders of magnitude. Noble gases that were evaluated as possible internal standards included neon, argon, and krypton.

Test mixtures and calibration standards

Several different types of gas and liquid mixtures and selected pure components in these mixtures were used to evaluate the performance of the columns listed in Tables III and IV. Table V shows the composition of the three different standard mixtures that were used to compare the performance of various columns. The hydrocarbon and oxygenate standards collectively contained nearly all of the important C_1–C_4 alkanes, olefins, acids, aldehydes, and ketones that have been reported as primary or secondary products in C_4 hydrocarbon oxidations (14–29).

The pure gas and liquid components used to check retention times and to prepare the standards were obtained from commercial sources. They were used as received without any further pretreatment. The gas mixture calibration standards were also obtained from two separate commercial sources. The liquid mixture calibration standards were prepared by a gravimetric technique with use of an electronic pan balance with a stated accuracy of ± 0.0001 g and a precision of ± 0.005 g. To minimize weighing errors during preparation of the standard because of volatility, the components were maintained in a chemical refrigerator and placed in a bed of dry ice during transfer to a cooled volumetric flask. Chilled acetone was used as a solvent based on solubility considerations. Binary solutions that contained between 1 and 8 wt% of maleic anhydride in acetone were also used to check for response linearity by using either a constant or variable manual injection volume once the preferred capillary column was identified.

These same mixtures were also used to evaluate both absolute and relative response factors for the appropriate detector. In some cases, manual injections of pure compounds or binary mixtures were used to determine either absolute or relative retention times.

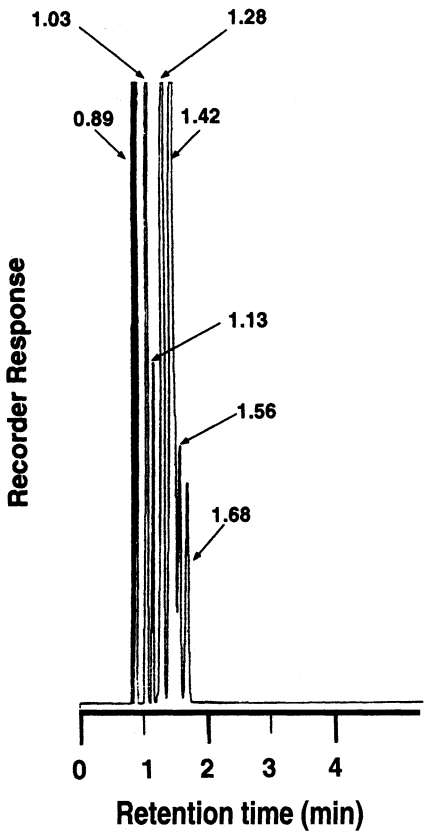

Figure 2. Chromatogram of the C_1–C_4 hydrocarbon gas standard obtained with the thick-film DB-1 column. Chromatographic conditions: column, 30 m x 0.53-mm i.d.; d_f, 5 µm carrier gas, helium at 10 sccm; split ratio, 40:1; 0.5 cc manual injection; electrometer range, 3; injector, 230°C; detector, 250°C; temperature program, 35°C for 12 min, 20°C/min to 100°C, hold 11.5 min, 20°C/min to 165°C, then hold 8 min.

Method description

A flow diagram of the final method is shown in Figure 1. Column 1 on the FID side is a 30-m × 0.53-mm i.d. bonded polydimethyl siloxane (DB-1; J&W Scientific, Folsom, CA), and column 2 is a 30 m × 0.53-mm i.d. Al_2O_3/KCl PLOT (Chrompack, Raritan, NJ). Both columns are mounted in the oven and connected to a six-port Valco switching valve so that the carrier gas flows through either DB-1 only or the DB-1 and Al_2O_3/KCl PLOT in series. The Al_2O_3 KCl/PLOT gives the

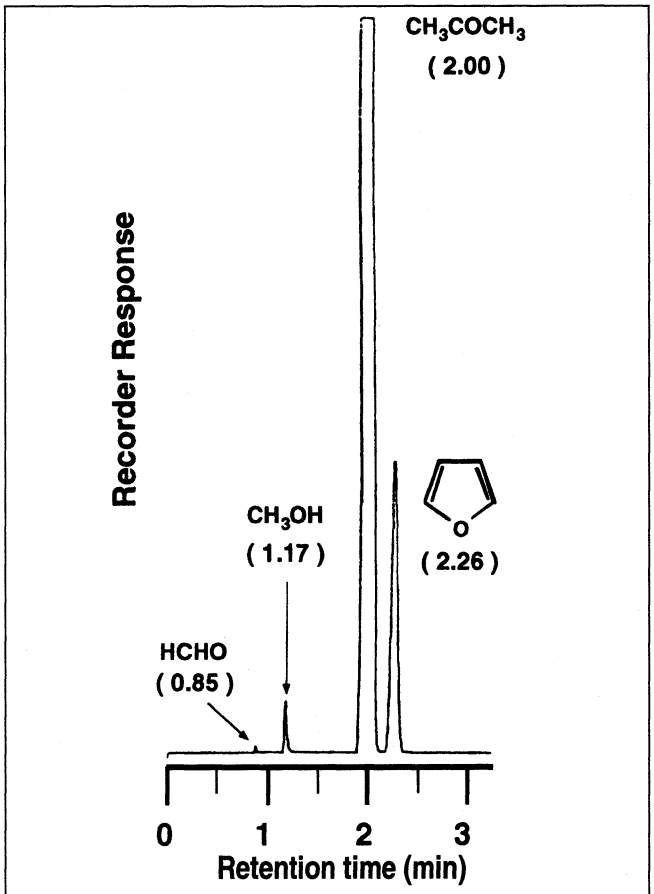

Figure 3. Chromatogram of the first eluting oxygenates from the DB-1 column used to determine the switching time of valve 2 for isolation of the C_1–C_4 hydrocarbons on the Al_2O_3/KCl PLOT column. Chromatographic conditions: column, 30 m x 0.53-mm i.d.; d_f, 5 µm carrier gas, helium at 10 sccm; split ratio, 40:1; 0.5 cc manual injection; electrometer range, 3; injector, 230°C; detector, 250°C; temperature program, 35°C for 12 min, 20°C/min to 100°C, hold 11.5 min, 20°C/min to 165°C, then hold 8 min.

Table VIII. Summary of Column Specifications and Overall Performance for Analysis of the Hydrocarbon and Oxygenate Standards

Column Type	Internal Diameter (mm)	Column Length (m)	Test Conditions	Comments
J&W DB-1 (d_f = 5 µm)	0.53	30	10 cc/min column flow rate; 40:1 split ratio; 35°C for 3.7 min, 10°C/min to 75°C, 20°C/min to 165°C	Good resolution for most species; some unsaturated acids peaks skewed
J&W DB-1 (d_f = 1.5 µm)	0.53	30	10 cc/min column flow rate; 40:1 split ratio; 35°C for 3.7 min, 10°C/min to 75°C, 20°C/min to 165°C	Adequate resolution for most species; significant peak skewness on all acids; MAN peak shape is satisfactory
J&W DB-5 (d_f = 1.5 µm)	0.53	30	10 cc/min column flow rate; 40:1 split ratio; 35°C for 3.7 min, 10°C/min to 75°C, 20°C/min to 165°C	Adequate resolution for most species; significant peak skewness on all acids; MAN peak shape is satisfactory
J&W DB-FFAP (d_f = 1 µm)	0.53	30	10 cc/min column flow rate; 40:1 split ratio; 35°C for 3.7 min, 10°C/min to 75°C, 20°C/min to 165°C	Excellent resolution of all species except MAN; symmetric peak shape with all acids; MAN does not elute
Restek 1701 (d_f = 3 µm)	0.53	30	10 cc/min column flow rate; 40:1 split ratio; 35°C for 3.7 min, 10°C/min to 75°C, 20°C/min to 165°C	Excellent resolution of nearly all species; symmetric peak shape with all species
Chrompack Al_2O_3/KCl PLOT	0.53	25	10 cc/min column flow rate; 40:1 split ratio; 35°C for 3.7 min, 10°C/min to 75°C, 20°C/min to 165°C	Very poor resolution of most oxygenates
			10 cc/min column flow rate; 11:1 split ratio; 35°C for 12 min, 20°C/min to 100°C	Excellent resolution of all C_1–C_4 hydrocarbons
Supelco 23% SP-1700 on 80/100 Chromosorb P AW	1/8*	30†	30 cc/min column flow rate; 70°C isothermal	Very poor resolution of all oxygenates; excellent resolution of all C_1–C_4 hydrocarbons
Chrompack PoraPLOT U	0.53	25	10 cc/min column flow rate; 40:1 split ratio; 35°C for 3.7 min, 10°C/min to 75°C, 20°C/min to 165°C	Very poor resolution of all oxygenates
Chrompack PoraPLOT Q	0.53	25	10 cc/min column flow rate; 40:1 split ratio; 35°C for 3.7 min, 10°C/min to 75°C, 20°C/min to 165°C	Partial resolution of oxygenates and hydrocarbons; some species result in skewed peaks

* This measurement given in inches.
† This measurement given in feet.

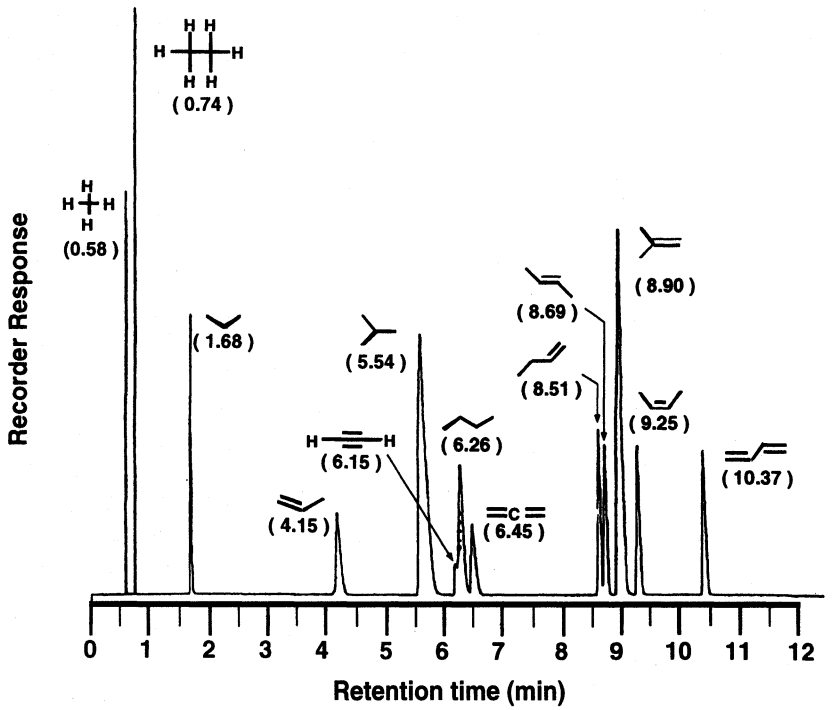

Figure 4. Chromatogram of the C_1–C_4 hydrocarbon standard using the Al_2O_3/KCl PLOT column. Chromatographic conditions: column, 30 m x 0.53-µm i.d.; d_f, 5µm carrier gas, helium at 10 sccm; split ratio, 40:1; 0.5 cc manual injection; electrometer range, 3; injector, 230°C; detector, 250°C; temperature program, 35°C for 12 min, 20°C/min to 100°C, hold 11.5 min, 20°C/min to 165°C, then hold 8 min.

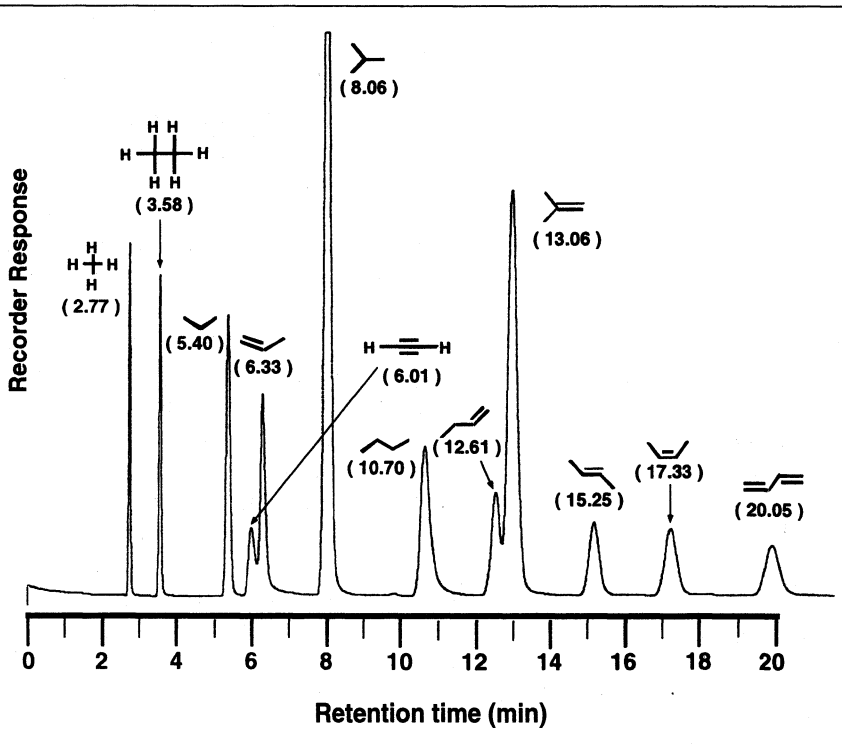

Figure 5. Chromatogram of the C_1–C_4 hydrocarbon standard obtained with the 23% SP-1700 on Chromosorb P AW column. Chromatographic conditions: column, 30 ft x 1/8-in. o.d.; carrier gas, He at 30 sccm; 0.5 cc manual injection; electrometer range, 3; injector, 230°C; detector, 250°C; temperature program, isothermal at 35°C.

method additional flexibility since it provides a baseline resolution of all C_1–C_6 hydrocarbons (73). This column is used when dehydrogenation or cracking of the *n*-butane to C_4 olefinic isomers and lower carbon number hydrocarbons is suspected.

The TCD side uses two stainless steel packed columns that are mounted in the same oven as the FID columns. Column 3 is 2 ft × 1/8-in. o.d. of 80/100 mesh Hayesep R, and column 4 is 10 ft × 1/8-in. o.d. of 60/80 mesh molecular sieve 5A. The columns are connected to a six-port Valco switching valve. The carrier gas is supplied from both a primary and a secondary source so that the flow is uninterrupted when the flow pattern is switched from a series to a parallel configuration. This eliminates undesired peaks that would otherwise occur with a conventional series-parallel column isolation method during temperature programming. It also results in a reduced overall analysis time since both columns are kept on-line. Coelution of different species from the two different columns does not occur because the relative retention times of all species that elute are sufficiently different to prevent peak overlap.

The temperature program that was used in the final method was primarily determined by the following factors: (*a*) the near coelution of CO_2 from the Hayesep R column with the O_2 from the molecular sieve column, which dictated the use of a low initial temperature so that these two species were resolved; (*b*) the need to preserve the peak shapes for H_2O and *n*-butane, which eluted from the Hayesep R column on the TCD side, as well as late-eluting carboxylic acids and maleic anhydride, which eluted from the DB-1 column on the FID side by using a high temperature programming rate; and (*c*) the similar retention times for formaldehyde, methanol, acetone, furan, and the C_1–C_4 hydrocarbon mixture on the DB-1 column, which made the split time for isolation of the hydrocarbons on the Al_2O_3/KCl PLOT column critical. These factors and the need to minimize total analysis time while maintaining resolution were taken into consideration; therefore, the columns were operated with the following temperature program: 35°C for the initial 6 min, increased to 75°C at 10°C/min, followed by another increase to 165°C at 20°C/min, with a final hold period of 5.5 min. Additional optimization of this temperature program to reduce the analysis time while maintaining or improving the peak characteristics might be possible but was not pursued during the course of this study.

Operation

The switching valve timing sequence that was used to obtain an on-line sample and to direct the carrier gas to the appropriate sequence of columns and detectors is summarized in Table VI. This version of the sequence assumes that the sample predominantly contains a single C_4 hydrocarbon, for example, *n*-butane, versus a more complex mixture of C_1–C_4 hydrocarbons so that only column 1 is used for resolution of the hydrocarbon–oxygenate mixture. The valve sequence was triggered by a 24-volt DC signal from the TI 545 process logic controller that was used for the reactor system automation.

With all valves in the off position (indicated by the solid lines in Figure 1), the flow diverter valve was switched to the on position so that the sample loops were filled by the reaction gas. After 2 min, this same valve was switched to the off position, and the gas samples were allowed to equilibrate for 0.3 min (18 s) before the sample valve was switched to inject the samples into columns 1 and 3 through column switching valves 1 and 2, respectively. Once the permanent gases and CO entered column 4 after passing through column 3 relatively unretained, valve 2 on the TCD side was switched so columns 3 and 4 operated in a parallel versus a series mode of operation. A continuous flow of helium was maintained through both columns with a common outlet to the TCD. At t = 4 min, the sample valve was switched back to the on position in preparation for the next sample. After the permanent gases and CO were eluted from column 4 and detected, the temperature was then programmed as described previously. After water and *n*-butane eluted from column 3, valve 2 was switched back after t = 17.9 min, which brought all valves back to the preinjection condition. All of the hydrocarbons and oxygenates were simultaneously eluted from column 1 and detected by the FID. All of the valve switching operations for the sample valve, valve 1, and valve 2 were controlled automatically by the HP 19405A Sample/Event Control Module from the data/event features of the HP 3396 integrator.

A modified form of the switching valve sequence for the FID side was implemented when the sample contained a more complex mixture of C_1–C_4 hydrocarbons, and a detailed analysis of these is required. This modification was necessary since column 1 alone could not provide baseline resolution for all of the C_1–C_4 hydrocarbon components and the oxygenated hydrocarbons in a single, temperature-programmed analysis that is compatible with the packed-column TCD method. The modified time versus event schedule is given in Table VII. Column 2 was incorporated into the sequence by switching valve 1 so that it was connected in series downstream of column 1 before the sequence was initiated. After the sample was injected, the hydrocarbons were allowed to elute from

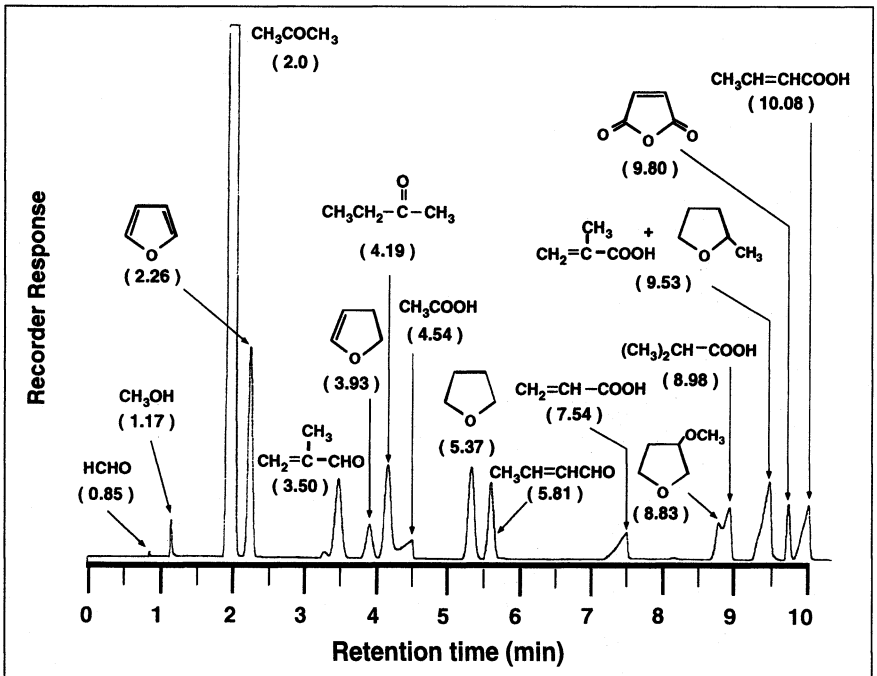

Figure 6. Chromatogram of the oxygenate liquid standard obtained with the DB-1 column with a film thickness of 5 µm. The chromatographic conditions are given in Table VIII.

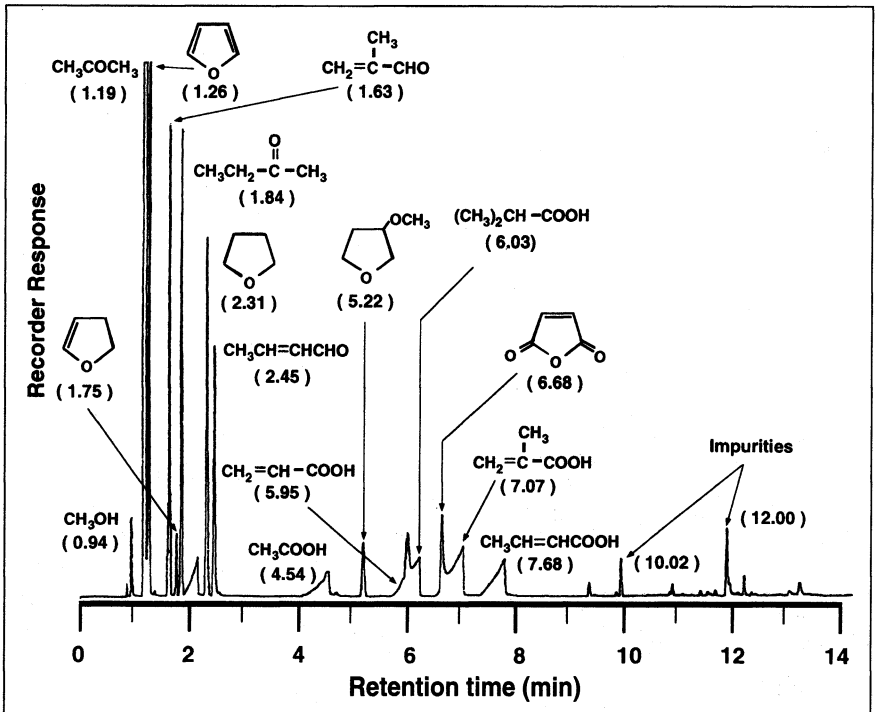

Figure 7. Chromatogram of the oxygenate liquid standard obtained with the DB-1 column with a film thickness of 1.5 µm. The chromatographic conditions are given in Table VIII.

column 1 onto column 2 before the first important oxidation byproduct, which is acetone, eluted onto column 2. Valve 1 was then switched to the on position (solid lines in Figure 1) to bypass column 2 until all of the oxygenates were eluted from column 2 and detected by the FID. The valve was then switched back to the off position, which placed columns 1 and 2 in series so that the hydrocarbons could be eluted from the latter column and detected by the FID. A needle valve restrictor was used in valve 1 so the carrier gas flow stayed constant through column 1 when column 2 was bypassed. The switching valve sequence for valve 2, which corresponded to the TCD, was unaffected and remained the same.

To determine the switching time for the modified form of the FID method where both column 1 and column 2 are used, the hydrocarbon standard was manually injected with valve 1 set at the off position so that the column effluent from column 1 was directed to the FID. A typical chromatogram is shown in Figure 2. The results indicate that the DB-1 column with a film thickness of 5 µm resolved some of the lighter hydrocarbons; 1,3-butadiene eluted last with a retention time of 1.68 min.

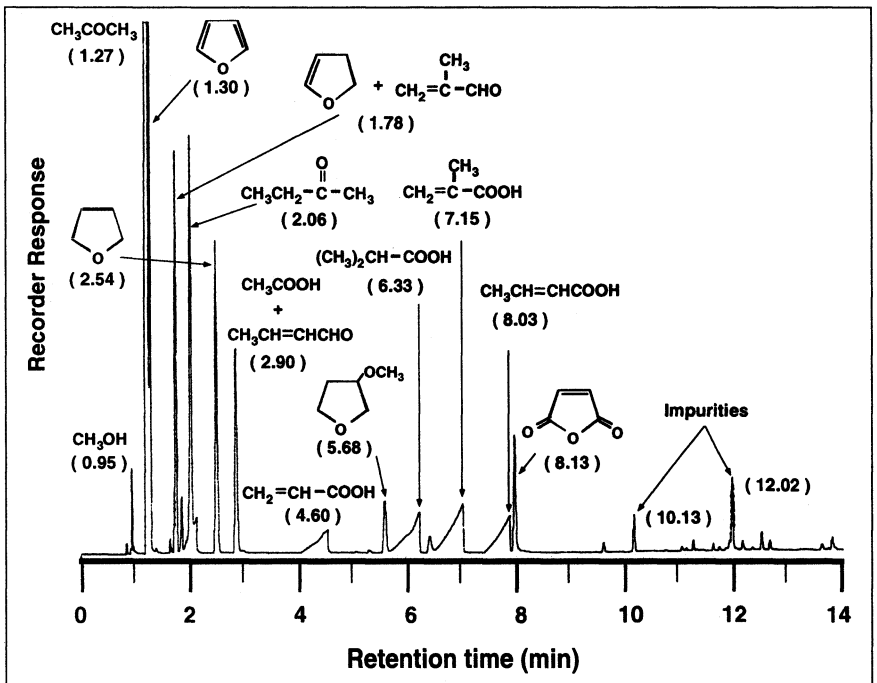

Figure 8. Chromatogram of the oxygenate liquid standard obtained with the DB-5 column with a film thickness of 1.5 µm. The chromatographic conditions are given in Table VIII.

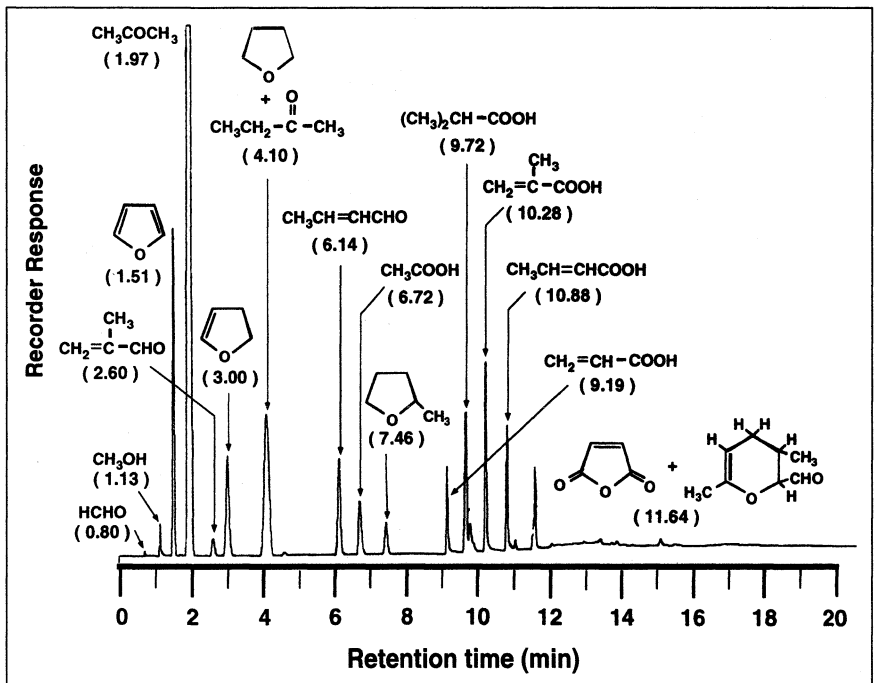

Figure 9. Chromatogram of the oxygenate liquid standard obtained with the Restek 1701 column with a film thickness of 3 µm. The chromatographic conditions are given in Table VIII.

Manual injection of the oxygenate standard yields the chromatogram in Figure 3 where only those components with a retention time of less than 2.3 min are shown. These components include formaldehyde at 0.85 min, methanol at 1.17 min, acetone at 2.0 min, and furan at 2.26 min. A comparison between Figures 2 and 3 suggested that a switching time between approximately 1.8 and 1.9 min would allow the hydrocarbons, formaldehyde and methanol, to be isolated in column 2 before the aldehydes, ketones, acids, and other remaining oxygenates eluted from column 1. Hence, a clean isolation between the hydrocarbons and oxygenated products was not possible unless a slightly lower initial temperature was used. Because formaldehyde and methanol are not typically produced in *n*-butane partial oxidations over vanadium-phosphorus catalysts under most commercial reaction conditions, the inability to isolate these two components was not viewed as being critical.

Once the precise value of the switching time was firmly established, the retention times for all of the major peaks were determined for subsequent peak identification in the Multichrom peak analysis data system. Retention time windows of ± 5% about the mean allowed all components to be reproducibly identified during routine application of the method.

Determination of the switching time for valve 2 of the TCD method was performed by using a procedure analogous to the one described for the FID method. Manual injections of CO_2 on column 3 and O_2 or air on column 4 were performed in separate experiments since these species eluted first from these columns. Since the retention time for CO_2 was slightly less than the

retention time for O_2, a first approximation to the valve switching time was determined by adding the retention time for CO_2 to the averaged difference between the retention times. Minor adjustments were then made after the columns were connected to the switching valve, and the permanent gas standard given in Table V was injected. Retention time windows of ± 5% of the mean allowed all components to be reproducibly identified during routine application of the method.

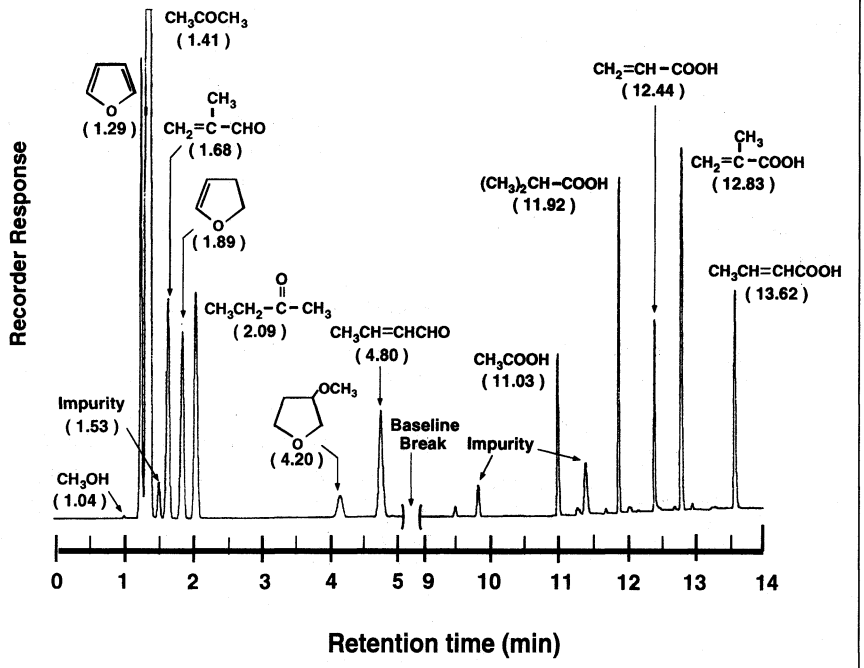

Figure 10. Chromatogram of the oxygenate liquid standard obtained with the DB-FFAP column with a film thickness of 1 µm. The chromatographic conditions are given in Table VIII.

Table IX. Comparison Between Normal Boiling Points (NBP) and Retention Times for the Key Components in the Chromatograms Shown in Figures 6–10

		Retention Time (min)				
Compound	NBP (°C)	J&W DB-1 5 µm	J&W DB-1 1.5 µm	J&W DB-5 1.5 µm	J&W DB-FFAP 1 µm	Restek 1701 3 µm
Methanol	64.7	1.17	0.94	0.95	1.04	1.13
Acetone	56	2.00	1.19	1.27	1.41	1.97
Furan	32	2.26	1.26	1.30	1.29	1.51
Methacrolein	69	3.50	1.63	1.78	1.68	2.60
2,3-Dihydrofuran	54.5	3.93	1.75	1.78	1.89	3.00
MEK	80	4.19	1.84	2.06	2.09	4.10
Acetic acid	117.5	4.54	4.54	2.90	11.03	6.72
Tetrahydrofuran	67	5.37	2.31	2.54	not obsd.	4.10
Crotonaldehyde	104	5.81	2.45	2.90	4.80	6.14
Acrylic acid	139	7.54	5.95	4.60	12.44	9.19
Isobutyric acid	153.5	8.98	6.03	6.33	11.92	9.72
Methacrylic acid	163	9.53	7.07	7.15	12.83	10.28
Maleic anhydride	202	9.80	6.68	8.13	not obsd.	11.64
Crotonic acid	180.5	10.08	7.68	8.03	13.62	10.88

Results and Discussion

Column evaluations: general comments

The columns listed in Table III were initially evaluated for resolution of the expected reaction products by manual injection of the synthetic hydrocarbon and oxygenate test mixtures whose compositions were given earlier in Table V. A summary of the test conditions used and abbreviated comments on the qualitative performance of each column is given in Table VIII. The Al_2O_3/KCl PLOT and 23% SP-1700 on Chromosorb P AW columns referred to in this table were not evaluated for resolution of the oxygenates, since their utility for separation of C_1–C_4 and C_1–C_6 hydrocarbons has already been demonstrated by the column manufacturers or in other literature (73). The ability of the remaining columns listed in Table VIII to provide baseline resolution of the synthetic oxygenate mixture used here has not been reported to our knowledge, however. Since the stationary phases in these columns represent a large range of relative polarities, a significant variation in column performance was expected. The qualitative and quantitative performance evaluation of each column on either the hydrocarbon or oxygenate standard is described in more detail below.

Column evaluations with the hydrocarbon standard

Chrompack Al_2O_3/KCl PLOT

The chromatogram for the Chrompack Al_2O_3/KCl PLOT column obtaining by using the hydrocarbon mixture is given in Figure 4. Baseline resolution of nearly all of the components was obtained, except for 1-butene at 8.51 min and *trans*-2-butene at 8.69 min, which have a slight overlap. The shoulder that appears on the leading edge of the *n*-butane peak at 6.15 min was identified to be acetylene by GC–MS in separate experiments. Ethylene was not present in this particular calibration mixture but would elute in the retention window between propane at 1.68 min and propylene at 4.15 min.

Supelco 23% SP-1700 on Chromosorb P AW

The chromatogram obtained with the Supelco 23% SP-1700 on Chromosorb P AW column is shown in Figure 5. When compared with the results obtained with the Chrompack Al_2O_3/KCl PLOT column, the peaks for the indicated species are clearly broader. This was expected because this is a classic ⅛-in. i.d. packed column that has a lower plate count than the megabore PLOT column. All of the species present in the hydrocarbon calibra-

tion mixture were identified, except for acetylene and propadiene. The peak on the leading edge of propylene at 6.33 min was believed to be acetylene, and it was surmised that propadiene must be coeluting with another species. It was noted that another peak was superimposed on *n*-butane in a separate injection performed at 70°C, which otherwise did not appear as a separate peak under temperature programmed conditions. This species is most likely propadiene. Since propadiene has not been reported or observed as a byproduct of *n*-butane oxidation, the inability of this column to resolve it is not a significant drawback from an applications perspective. The higher carrier gas flow rate required by this column, when compared with that of the megabore column identified for resolution of the oxygenate analysis, suggested that it was not suitable. In addition, the chromatogram in Figure 5 is based on an isothermal temperature of 35°C. This temperature would not be compatible with the temperature program needed to resolve the oxygenates on a more polar column, as illustrated below. However, any related multidimensional method that involves the use of packed columns with both the FID and TCD might be able to use this particular packing material for resolution of the hydrocarbons.

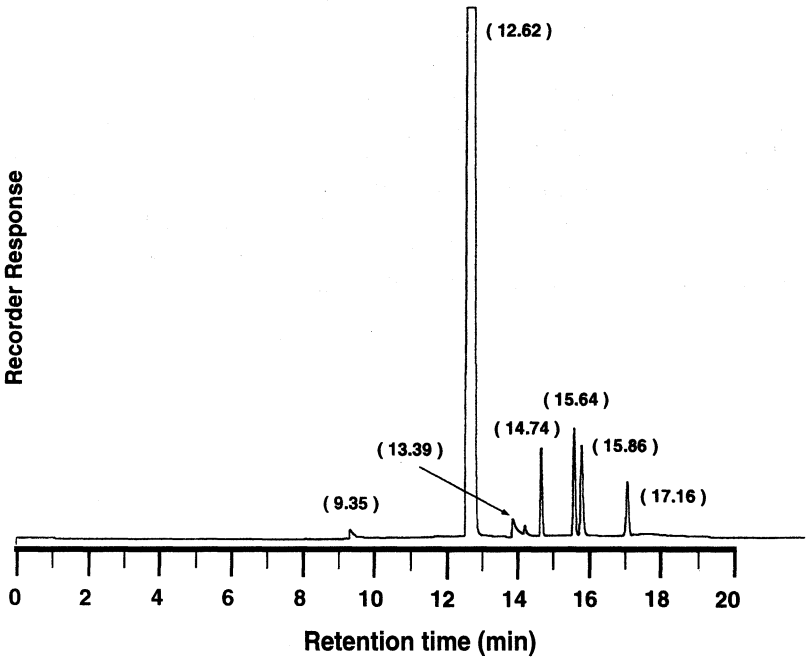

Figure 11. Chromatogram obtained when the oxygenate standard was analyzed with the Poraplot Q column.

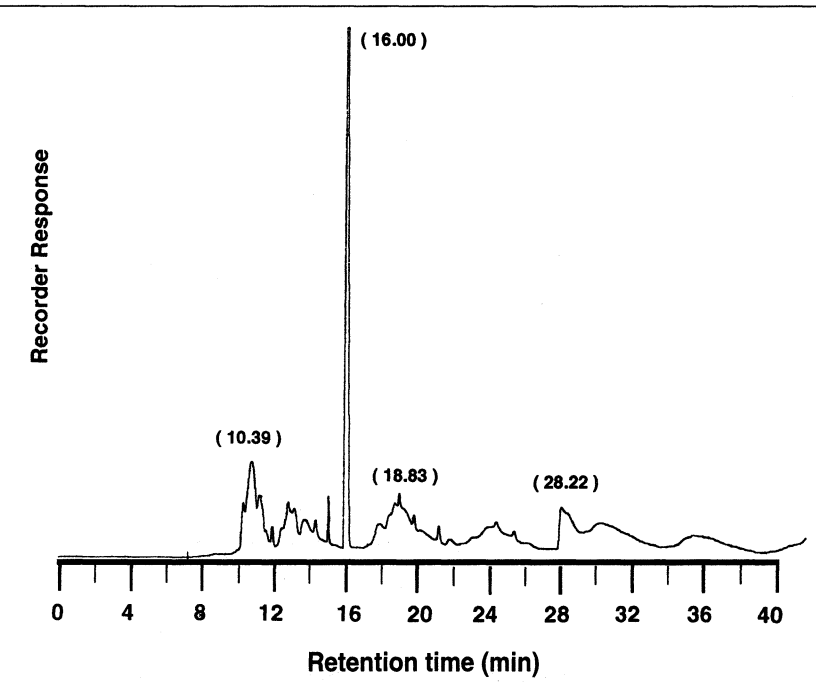

Figure 12. Chromatogram obtained when the oxygenate standard was analyzed with the Poraplot U column.

Column evaluations by using the oxygenate standard

J&W DB-1 thick-film column

The chromatogram obtained when the oxygenate standard was analyzed by using the thick film (d_f = 5 µm) nonpolar DB-1 column is shown in Figure 6. Most of the components are baseline resolved, although several exceptions exist. The first peak overlap occurs between methyl ethyl ketone at 4.19 min and acetic acid at 4.54 min. Another peak overlap occurs between 2-methoxy tetrahydrofuran and isobutyric acid at retention times of 8.83 and 8.98 min, respectively. However, 2-methoxy tetrahydrofuran is an impurity present in the tetrahydrofuran and has not been reported as a reaction byproduct in butane oxidation to maleic anhydride (12,17,25,27–39). Hence, the resolution and quantitation of this component is not important. Finally, methacrylic acid and methyl tetrahydrofuran yield a composite peak at a retention time of 9.53 min. The latter species is also an impurity in the tetrahydrofuran. Resolution and quantitation of this component is also not important for reasons that are analogous to those given above for 2-methoxy tetrahydrofuran.

All of the possible organic acid byproduct components, namely, acetic acid at 4.54 min, acrylic acid at 7.54 min, isobutyric acid at 8.98 min, methacrylic acid at 9.53 min, and crotonic acid at 10.08 min, have unsymmetrical peaks with an elongated leading edge that is indicative of nonlinear solute adsorption. Symmetric peaks are obtained for furan at a retention time of 2.26 min and various related derivatives, such as 2,3-dihydrofuran at 3.93 min, tetrahydrofuran at 5.37 min, and 2-methoxy tetrahydrofuran at 8.83 min.

All of the aldehydes, ketones, and alcohols, such as formaldehyde at a retention time of 0.85 min, methanol at 1.17 min, methacrolein at 3.50 min, and crotonaldehyde at 5.81 min, were baseline resolved and resulted in symmetric peaks. Maleic anhydride, which is the desired reaction product in *n*-butane oxidation, appeared to be baseline resolved. It eluted as a symmetric peak at a retention time of 9.8 min, which is between the composite peak containing methacrylic acid and methyl tetrahydrofuran at 8.98 min, and the crotonic acid peak at 10.08 min.

J&W DB-1 thin-film column

The chromatogram shown in Figure 7 is also based on a nonpolar DB-1 stationary phase, except that a thinner film thickness (d_f = 1.5 µm) was selected to examine the effect of film capacity on peak shape. When compared with the chromatogram in Figure 6, the effect of the film thickness on the peak shapes and retention times is striking. As expected, the peaks in Figure 7 are more narrow since the film volume per unit column length for the thin film column is a factor of 18 less than that for the thick film column. Hence, the characteristic time for diffusion of the solute into the thin film was reduced. The retention times for all components were also less, but the elution order of all components was otherwise identical to that obtained with the thicker film DB-1 column.

Close inspection of the chromatogram for the thin-film DB-1 column shows that some of the key components were not baseline resolved and that unsymmetric peak shapes are present. For example, a composite peak was obtained for acrylic acid and isobutyric acid at retention times of 5.95 and 6.26 min, respectively. An impurity, which is most likely methyl tetrahydrofuran, eluted between these latter two species. Another composite peak was obtained for maleic anhydride and methacrylic acid at retention times of 6.68 and 7.07 min, respectively. All of the peaks associated with the acids were unsymmetric, while peaks associated with the ketones and

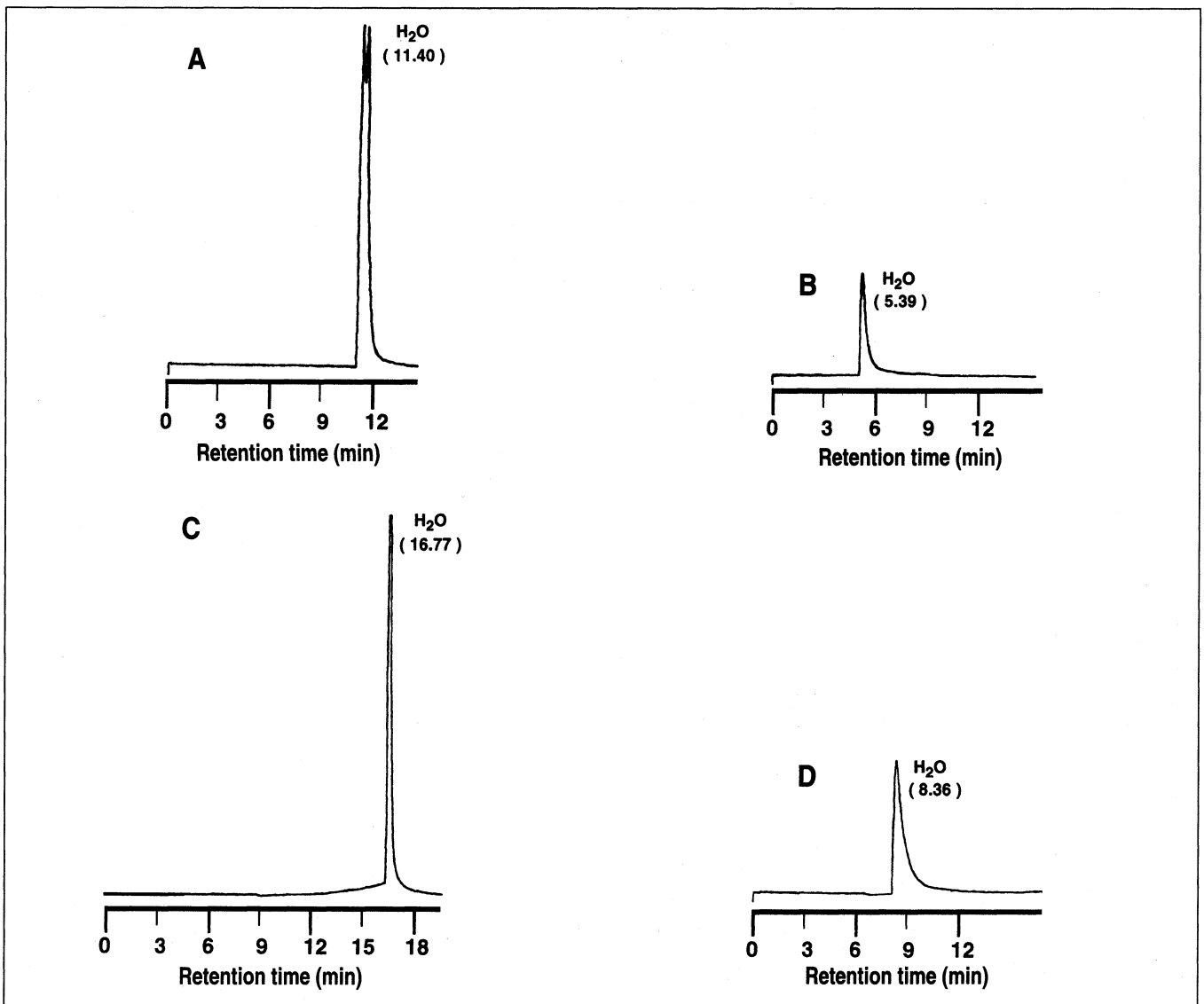

Figure 13. Comparison of water peaks obtained from various packed columns: A, Hayesep A; B, Hayesep D; C, Hayesep T; D, Porapak QS. Chromatographic conditions: carrier gas, helium at 30 sccm; 0.5 cc manual injection; detector, thermal conductivity; range, 1; high sensitivity; injector, 230°C; detector, 250°C; temperature program, 35°C for 12 min., 20°C/min to 100°C, hold 11.5 min, 20°C/min to 100°C, then hold 8 min.

aldehydes were symmetric. This behavior is analogous to that observed for the thick-film DB-1 column.

J&W DB-5 thin-film column

Figure 8 shows the chromatogram obtained when the oxygenate standard was analyzed by using the slightly polar DB-5 column with a thin film (d_f = 1.5 µm). This particular stationary phase, which is slightly more polar than DB-1, resulted in peak overlap between the following binary components: acetone at 1.27 min and furan at 1.30 min; 2,3-dihydrofuran and methacrolein at 1.78 min; and acetic acid and crotonaldehyde at 2.90 min. Unsymmetric peaks were observed for all of the baseline-resolved acid components, which was identical to that observed for both the thin-film and thick-film DB-1 columns. Maleic anhydride eluted after crotonic acid at a retention time of 8.13 min, which was opposite to that observed for the DB-1 column. The ability of the DB-5 column to resolve the oxygenate mixture generally appeared to be inferior to that of the DB-1 column with the thick film (d_f = 5 µm), at least for the particular temperature program used here. While other temperature programs could conceivably lead to better resolution, the one used here was compatible with the temperature program needed to resolve the components analyzed by the method on the TCD side.

Restek medium-film column

Figure 9 shows the chromatogram obtained when the oxygenate standard was analyzed using the Restek 1701 column. This stationary phase was more polar than either the DB-1 or DB-5 phases but less polar than the DB-FFAP phase. All of the peaks were symmetric, and baseline resolution of almost all components was obtained. Mass spectrometry analysis showed that methyl ethyl ketone and furan coeluted at a retention time of approximately 4.1 min. Also, the leading edge of the maleic anhydride peak at 11.64 min overlapped with another peak at 11.59 min that was identified by mass spectrometry as 2,3-dihydro-2,5-dimethyl-2H-pyran-2-carboxaldehyde. This latter species was identified in separate GC–MS injections as a small impurity in the methacrolein that was used to prepare the oxygenate standard. Fortunately, it was neither an expected nor an observed byproduct from the partial oxidation of *n*-butane from

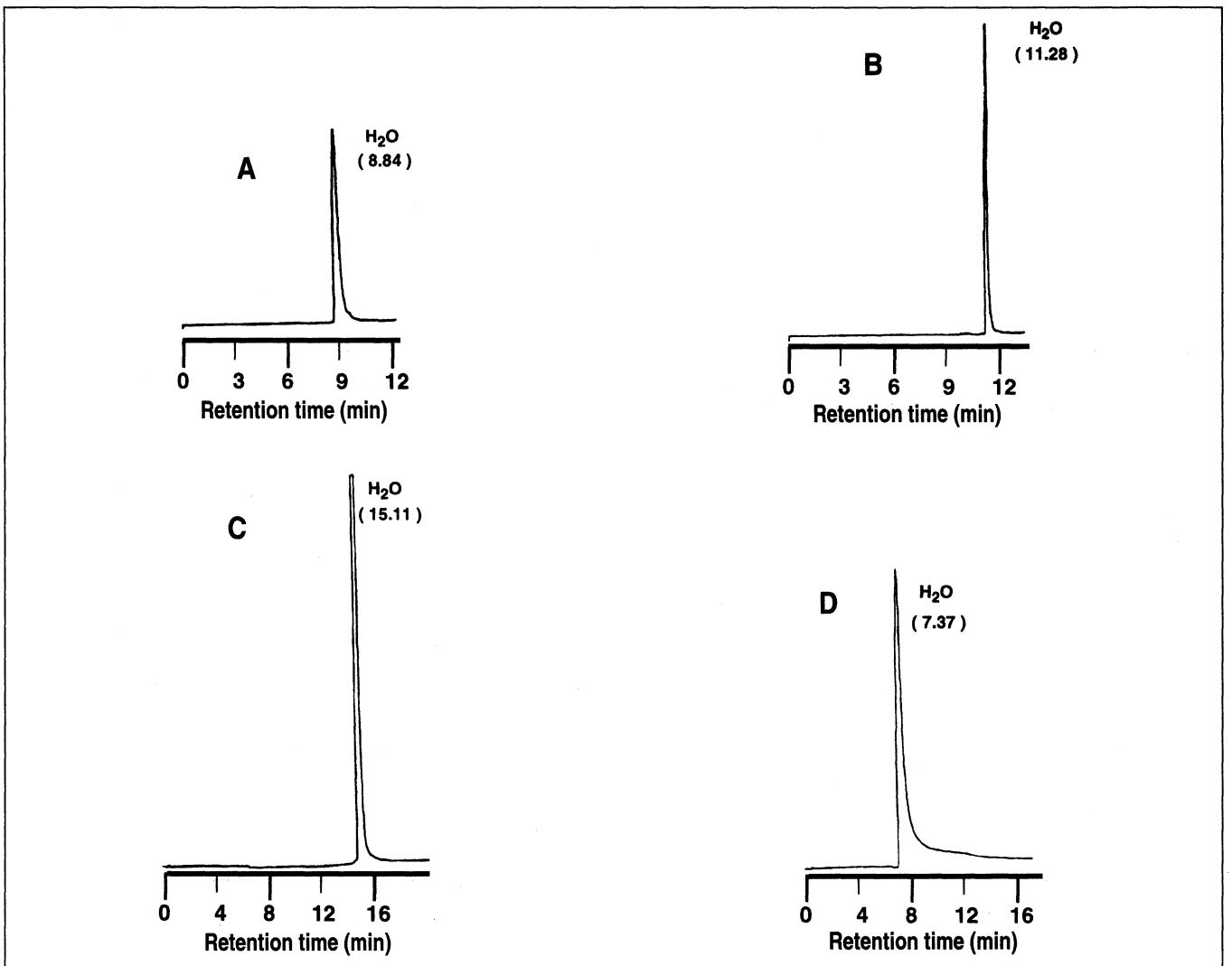

Figure 14. Comparison of water peaks obtained from various packed columns: A, Hayesep R; B, Hayesep R; C, Hayesep Q; D, Chromosorb 102. Chromatographic conditions: carrier gas, He at 30 sccm; 0.5 cc manual injection; detector, thermal conductivity; range, 1; high sensitivity; injector, 230°C; detector, 250°C; temperature program, 35°C for 12 min, 20°C/min to 100°C, hold 11.5 min, 20°C/min to 100°C, then hold 8 min.

maleic anhydride. Hence, it would not be present in the product gas obtained from a typical catalyst evaluation experiment so that assignment of maleic anhydride to the peak at the indicated retention time would be accurate.

Unlike the results produced from the DB-FFAP column, maleic anhydride did indeed elute from this particular column and yielded a symmetric peak. Another distinct feature when compared with the DB-FFAP column was that the differences between retention times of the various components were more uniform, especially in the retention time window between approximately 5 and 10 min.

J&W DB-FFAP thin-film column

The ability of the polar DB-FFAP column with a film thickness of 1 µm to resolve the oxygenate mixture is illustrated in Figure 10. When compared with the previous chromatograms in Figures 6–9 that were obtained with the less polar DB-1, DB-5, and Restek 1701 stationary phases, the results are quite different. All of the peaks, including those associated with the C_1–C_4 acids, were symmetric with baseline resolution for nearly all components, except for the near-baseline resolution of furan at a retention time of 1.29 min and acetone at a retention time of 1.41 min. This represented a marked improvement over the relatively nonpolar DB-1 and DB-5 columns. Although these particular features are attractive, a significant disadvantage for this particular application is that maleic anhydride did not elute under these particular chromatographic conditions. Irreversible adsorption of the maleic anhydride apparently occurred with the DB-FFAP stationary phase. For this reason, it was not suitable for analysis of *n*-butane partial oxidation reaction products. However, this particular column would be an excellent choice for analysis of isobutylene or isobutane partial oxidation reaction products, since many of the species shown in Figure 9 are primary or secondary products of this reaction, except for maleic anhydride.

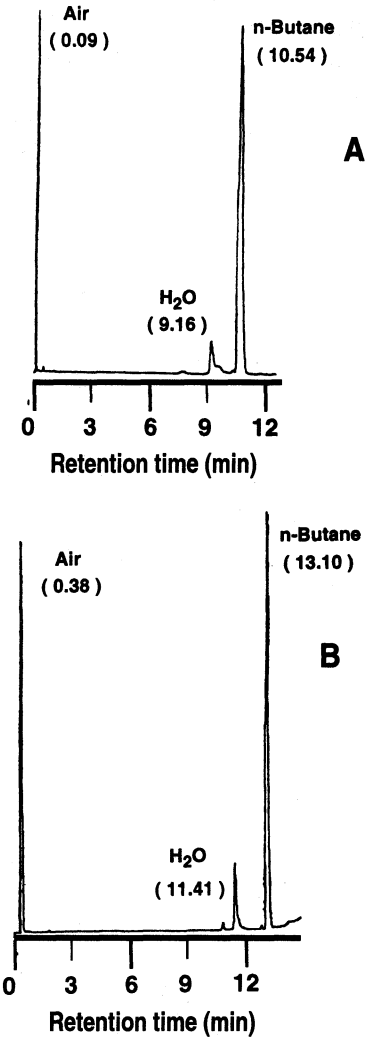

Figure 15. Effect of column length on the air, water and *n*-butane peaks obtained from two columns containing Hayesep R packing: A, length = 2 ft; B, length = 6 ft. Chromatographic conditions: column, $^1/_8$-in. o.d.; carrier gas, helium at 30 sccm; 0.5 cc manual injection; thermal conductivity detector; range, 1; high sensitivity; injector, 230°C; detector, 250°C; temperature program, 35°C for 12 min, 20°C/min to 100°C, hold 11.5 min, 20°C/min to 100°C, then hold 8 min.

Table IX shows a comparison of the retention time of the various oxygenated species for the various columns that were tested and their respective normal boiling points. It shows that the component elution order does not directly correlate with an increase in the normal boiling point. However, a direct correlation does exist within a specific class of compounds, for example, the furan derivatives, olefinic acids, and olefinic aldehydes. Maleic anhydride is an anomaly in this sense, since it eluted either before or after crotonic acid depending on the stationary phase used, even though the normal boiling point of the latter species is lower by more than 20°C.

The elution order of the various components from the DB-FFAP column in Table IX shows that the retention times can be correlated with the boiling points, if the comparison is made within a given group of acids, aldehydes, or ketones.

Other columns

The chromatograms obtained by using the remaining columns listed in Table III, such as the Poraplot Q and Poraplot U columns, are shown in Figures 11 and 12, respectively. Generally, these columns resulted in poor resolution of the oxygenate mixture when the evaluations were conducted with the same temperature program used above. Although modified temperature programs improved the resolution, the results were generally still inferior to those obtained with columns based on the DB-1, DB-FFAP, and the 1701 stationary phases. The use of these particular Poraplot columns for exploratory butane oxidation catalyst research where a variety of byproducts could be produced may result in peak overlap and possible misidentification of the reaction products unless detailed mass spectrometry is performed on each sample. For the purposes of this work in which a simultaneous analysis was performed on the TCD side, the temperature program required for satisfactory operation of the Poraplot Q column would be incompatible.

Column evaluations using the permanent and combustion gas standards

The various packed columns listed in Table IV were initially evaluated for resolution of oxygen, nitrogen, CO, CO_2, water, and

n-butane by manual injection of the pure components and selected mixtures. The basic approach was to identify a packing that would retain the more polar components (CO_2, water, and *n*-butane) while allowing the remaining components (O_2, N_2, and CO) to pass through relatively unretained. Since molecular sieves, such as molecular sieves 5X and 13A, are well-known for their ability to resolve the latter three species based upon size exclusion, the primary challenge was to identify a packing that would resolve CO_2, *n*-butane, and water while giving a high quality, symmetric peak shape. It was expected that the remaining higher molecular weight components, such as maleic anhydride and possible byproduct oxygenates, would be either irreversibly adsorbed or could be selectively removed using an appropriate guard column. Performance comparisons of each column are given below using selected species to illustrate the key results that were used to develop the final multidimensional system.

Hayesep porous polymer columns

Figures 13 and 14 show the water peaks obtained with use of a series of manual injections and the Hayesep porous polymer columns listed in Table IV. The particular conditions used are given in the figure caption. All columns contained 80/100 mesh packing with column lengths of 2–6 ft, except for one Hayesep A column where 100/120 mesh was used. Two of the columns, which contained Hayesep A (Figure 13A) and Hayesep D (Figure 13B), resulted in water peaks with noticeable tailing when compared with the results with Hayesep Q (Figure 14C), Hayesep R (Figures 14A and 14B), and Hayesep T (Figure 13C), so these packings were not investigated further. The water peak shapes from Hayesep Q and Hayesep T appeared to be acceptable, but the retention times were noticeably longer when compared with those obtained with Hayesep R. The retention time of water for the latter three packings generally increased in the following order: Hayesep T > Hayesep Q > Hayesep R at a constant column length of 5–6 ft. A short (2-ft) section of Hayesep R produced a nearly symmetric water peak with a retention time of approximately 9 min. This was within an acceptable retention window for CO_2 and *n*-butane, which were the other two species that are resolved on this column.

Figure 15 shows the peaks obtained when a mixture of 5% *n*-butane in moist air was injected into two Hayesep R columns with lengths of 2 and 6 ft, respectively. The retention times of

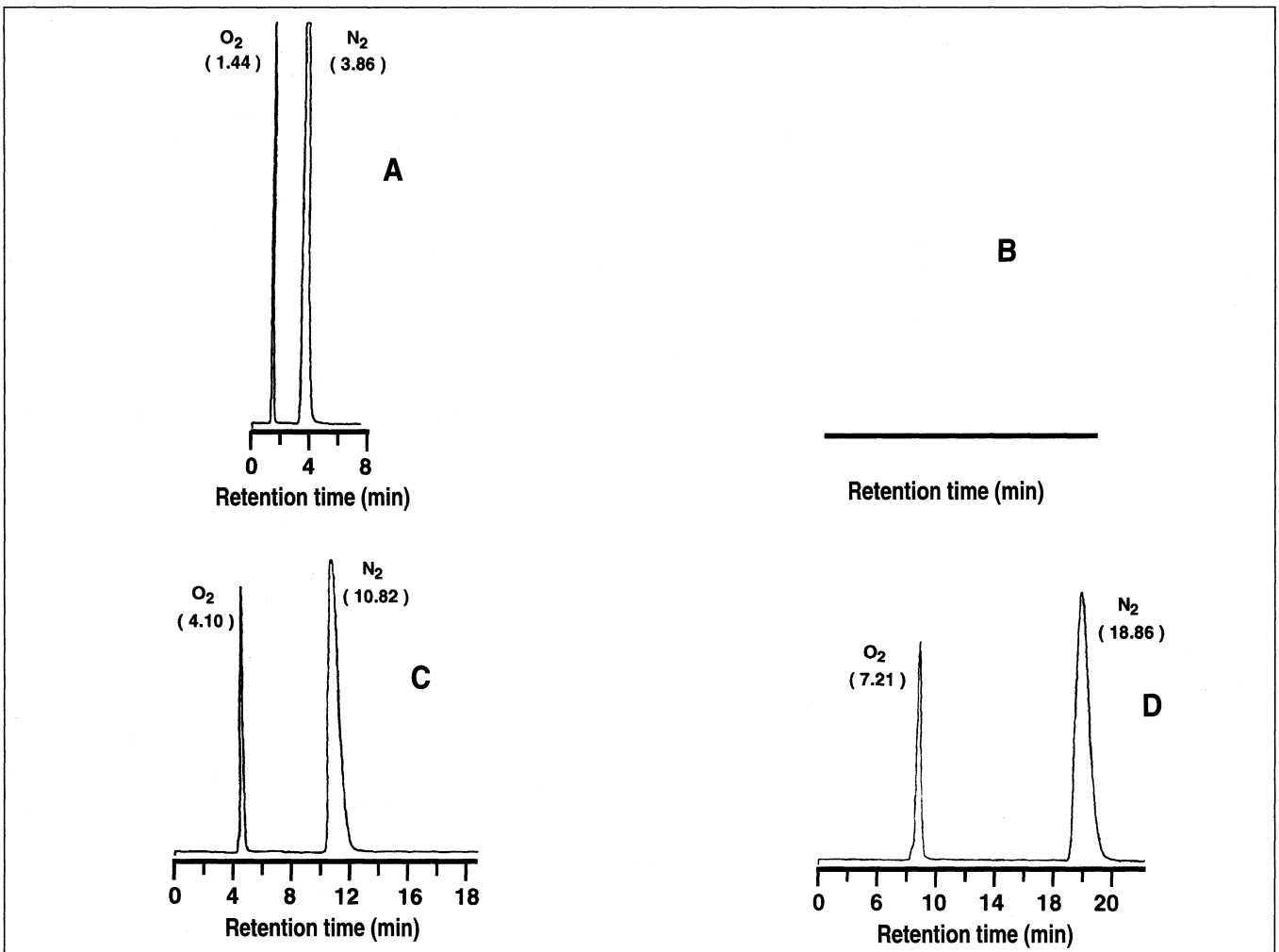

Figure 16. Effect of column length on the oxygen and nitrogen peaks obtained from various columns containing molecular sieve 5A packing: A, length = 6 ft; B, length = 12 ft; C, length = 13 ft; D, length = 14 ft. Chromatographic conditions: column, 1/8-in. o.d.; carrier gas, helium at 30 sccm; 0.5 cc manual injection; detector, thermal conductivity; range, 1; high sensitivity; injector, 230°C; detector, 250°C; temperature program, 35°C for 12 min, 20°C/min to 100°C, hold 11.5 min, 20°C/min to 100°C, then hold 8 min.

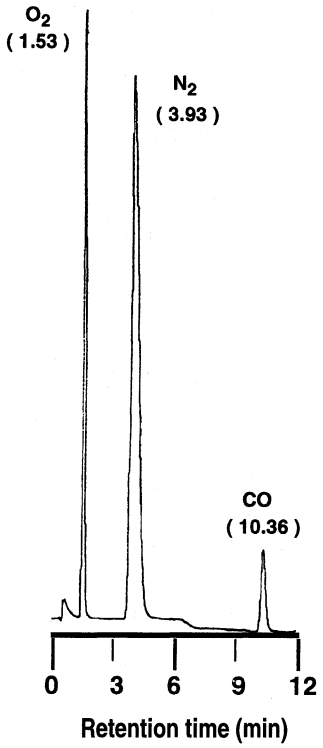

Figure 17. Separation of air and CO using argon as the carrier gas. Conditions: 35°C for 6 min, 20°C/min to 170°C; range, 1; high sensitivity; 30 cc/min; injector, 230°C; detector, 250°C.

Table X. TCD Area Counts and Absolute Response Factors for *n*-Butane in Nitrogen

Injection no.	TCD area counts for *n*-Butane 1%	2%	4%
1	903,127	1,729,890	3,439,597
2	884,690	1,721,633	3,435,683
3	898,906	1,727,567	3,429,185
4	896,397	1,726,441	
5	898,748		
6	900,486		
Average for butane	897,059	1,726,383	3,434,822
Average for nitrogen	13,408,228	13,187, 874	13,155,477
Standard deviation	6454	3477	5259
Standard deviation (% of average)	0.72	0.2	0.15
Absolute response, f (μV-s/μmol)	6,969,192	6,696,454	6,661,653
Absolute response for N_2 (μV-s/μmol)	1,050,689	1,043,966	1,063,098
Relative response, N_2 reference	6.62	6.41	6.27

* Note: The sample loop parameters were a temperature of 473 K, a pressure of 1 atm, and a volume of 500 μL. The calibration gas was 1, 2, and 4 mol% of *n*-butane in N_2 (three mixtures). The gas flow rate was 50 sccm at 21°C and 1 atm.

n-butane for these two different lengths were 10.5 and 13.1 min, respectively. As shown earlier in Figure 14A, the retention time for water on the 2-ft Hayesep R column was 8.84 min, so the difference in retention times for *n*-butane and water was 10.5 – 8.8 = 1.7 min. Hence, these two species can be adequately resolved on this column. Inspection of Figure 15 also shows that air was unretained on the polar Hayesep R packing so it can be trapped on a molecular sieve column that is located downstream. A similar result was obtained when a mixture of CO and air was used. Based upon these results, the 2-ft section of Hayesep R was selected as the initial column of choice for resolution of CO_2, water, and *n*-butane.

Porapak and Chromosorb columns

A few limited evaluations were performed to assess the resolution of water on packed columns containing Chromosorb and Porapak supports. The particular ones examined here were Chromosorb 102 and Porapak QS, since these were used as part of the GC analytical method described in several previous studies on kinetic studies of *n*-butane oxidation to maleic anhydride over vanadium-phosphorus oxide catalysts (39,70,71).

Figure 13D shows that a 6 ft × ⅛-in. o.d. Porapak QS column gives a water peak with a retention time of 8.36 min, which is similar to the retention time of 8.84 min obtained with the 2-ft × ⅛-in. o.d. Hayesep R column. However, the peak shape obtained from the Porapak QS column had more pronounced tailing when compared with that obtained with the shorter Hayesep R column, so the Porapak QS packed column would not be preferred in this application.

Figure 14D compares the water peak from a 6 ft × ⅛-in. o.d. Chromosorb 102 column with those produced by manual injections with the Hayesep R (Figures 14A and 14B) and Hayesep Q (Figure 14C) columns. It is evident that use of the Chromosorb 102 column resulted in pronounced peak tailing and the results were also inferior.

Although more evaluations could be performed with other packings of this type, the literature review given in the previous section and the results of the above studies indicate that the Hayesep porous polymer packings are preferred for the resolution of CO_2, water, and *n*-butane.

Molecular sieve columns

Packed columns based upon molecular sieves 5A and 13X are well-known for their ability to resolve CO and air and have been widely used in the GC analytical methods for *n*-butane oxidation reactor systems (31,32,39,63,67,69,71). The column length needed to prevent overlap of oxygen eluting from the molecular sieve column with CO_2, which was the first component to elute from the Hayesep R column, was experimentally determined as explained below.

Figure 16 compares the chromatograms

obtained when air was injected into various ⅛-in. o.d. molecular sieve 5A columns with lengths between 6–14 ft. As expected, increasing the column length led to a proportional increase in both the retention time difference between oxygen and nitrogen and the peak widths at half-height. These results suggested that overlap with CO_2 eluting from the Hayesep R column could be prevented by using a column length of 10 ft. The retention time of CO, which is the last eluting component from the molecular sieve column (not shown), was approximately 8.75 min in the final method, which was within the desired 15-min total analysis time.

Argon carrier gas

A limited investigation was performed to assess the use of argon as a carrier gas on the TCD side as a substitute for helium carrier gas. The motivation for using argon as a carrier gas was to reduce the magnitude of the nitrogen peak so that the peak maximum for nitrogen would not saturate the TCD, and reliable peak integration and quantitation could be obtained. Saturation of the TCD by nitrogen occurred since it was present at a concentration of approximately 75 mol% when butane oxidation catalyst testing was performed in the lean mode where the concentration of the reactor feed gas was between 1.5 and 2% *n*-butane in air. All other species that were detected on the TCD side, such as O_2, CO, CO_2, water, and *n*-butane, were present at sufficiently low concentrations that their peak maximums did not saturate the TCD when it was operated at a range of unity and at a high sensitivity setting. The ability to quantitate nitrogen with both precision and accuracy was considered important since this species was present in the feed gas at a known composition and was inert to the catalytic reaction processes. Hence, nitrogen was considered a possible internal standard or reference species for use in subsequent evaluation of response factors for the remaining species.

Figure 17 shows a typical TCD output obtained when the permanent gas standard was injected into a 6 ft × ⅛-in. o.d. packed column that contained a 60/80 mesh molecular sieve with argon carrier gas. The peak maximum of the nitrogen peak was smaller than the peak maximum for oxygen, which is the exact opposite of the situation shown above in Figure 16A where air was separated using helium as the carrier gas. Hence, reliable quantitation of nitrogen was possible since it did not saturate the TCD. However, the drawback of using argon as a carrier gas was that the relative sensitivities of other key species that were detected by the TCD, such as CO, CO_2, water, and *n*-butane, were decreased when compared with the relative sensitivities obtained by using helium as the carrier gas. Quantitation of these species, which are often present at low concentrations (e.g., less than 5 mol%) in the reactor product gas, was less reliable. For this reason, the use of argon as a carrier gas was not pursued. The use of argon or neon as an internal standard in the reactor feed gas at a concentration between 3–10 mol% was shown in later work to be the preferred approach. Also, reliable quantitation of nitrogen was possible with helium carrier gas, even though the TCD output showed that it was beyond the saturation value. Cases where the nitrogen concentration was varied from the normal value in air but still resulted in saturation of the TCD were not considered as reliable data, however.

Table XI. TCD Area Counts and Absolute Response Factors for the Permanent Gas and Combustion Gas Standard*

	TCD Area Counts			
Injection No.	Nitrogen	Oxygen	Carbon Monoxide	Carbon Dioxide
1	20,074,814	5,423,869	497,505	532,575
2	18,225,488	5,433,041	451,333	539,752
3	20,144,535	5,458,914	454,565	542,593
4	20,248,248	5,395,126	448,493	532,533
5	20,118,980	5,441,572	453,900	552,070
6	20,147,922	5,427,142	456,037	552,678
7	20,075,010	5,419,122	456,942	549,408
8	20,111,690	5,415,269	453,982	549,598
9	19,880,838	5,375,901	444,608	538,498
Average	19,891,947	5,421,106	457,485	543,301
Standard deviation	632,482	24,473	15,501	7976
Standard deviation (% of average)	3.18	0.45	3.39	1.47
Absolute response, f	2,052,094	2,116,547	3,658,836	4,092,048
Relative response, N_2 reference	1	1.03	1.78	1.99
Relative response, (75)	1	1.04	1	2.15

* The sample loop conditions were a temperature of 473 K, a volume of 500 µL, and a pressure of 1 atm. The calibration gas was 0.97% CO, 1.03% CO_2, 2.93% Ar, 75.2% N_2, 19.87% O_2.

Response factors and calibration

A series of experiments were performed with the gas and liquid calibration standards listed in Table V to determine both absolute and relative TCD and FID response factors for the key reaction species. A knowledge of these factors and their statistical characterization is essential when standard measures of the reactor and catalyst performance, such as reactant conversions, product selectivities, product yields, and reaction kinetic parameters, are derived from the raw GC peak areas of each species. A survey of recent publications that consider catalytic or engineering aspects of *n*-butane oxidation over vanadium–phosphorus metal oxide catalysts shows that numerical values for the response factors are not reported (29–39). In addition, statistical characterization of the response factors is not provided, so that errors associated with the derived catalyst performance parameters and other related quantities cannot be assessed. This section summarizes the response factors derived from experimental data using various calibration standards and other streams of known composition.

TCD response factors

Table X shows the area counts from the TCD for repeated injections of a gas stream containing either 1, 2, or 4 mol% *n*-butane in nitrogen. These compositions were obtained by diluting a flowing stream containing 10 mol% *n*-butane in nitrogen from a commercial gas blend with a separate stream of nitrogen using the mass flow controllers that are part of the reactor feed manifold. The proper mass flow controller set points were determined by direct measurement of the individual streams with several replicates using an optical soap-bubble meter that was attached to a calibration port. The injections were performed on-line by using the 10-port sampling valve as previously shown in Figure 1. For this latter reason, the results would be representative of those obtained during a typical catalyst testing experiment with on-line analysis.

The standard deviation of the area count in Table X at a fixed value for the butane composition is generally less than 1% of the averaged area count. The data for the 4 mol% *n*-butane composition was based only on three replicates. However, it produced a standard deviation that was similar to those obtained for the other two compositions, even though the latter results were based on a greater number of replicates. The ability of the method to provide repeatable results is attractive for catalyst testing applications where rapid turnaround is needed, such as initial screening of new catalyst compositions, since only a few replicates may be necessary to have an acceptable standard deviation.

Table XI compares the TCD area counts for different species that were obtained from repeated injections of the permanent gas and combustion gas standard whose composition is given in Table V. These were obtained by following the same procedure described above for *n*-butane, except nitrogen was not used as a dilution gas, since it was already present in the calibration gas mixture. The standard deviation of the area count for CO was within 3.34% of the average value, while those for the remaining species were between this value and 0.45%. The relative molar response factors for each species with nitrogen as a reference species were reasonably close to those derived using tabulated values given by Dietz (74). An exception was the relative response factor for CO, which differed from the literature value by about a factor of 2. Repeating this exercise with gas calibration mixtures from the same and different commercial sources yielded similar results, so the indicated value was deemed to be within acceptable experimental error and used in all subsequent calculations.

Table XII shows the data used to determine the TCD response factor for water. These were obtained by pumping a liquid solution containing approximately 10% water in acetone at 1.54 mL/h into the reactor system vaporizer along with nitrogen carrier gas. The resulting vaporized feed gas was then sampled on-line by using the sampling valve system described earlier in Figure 1 every 30 min. The standard deviation was within approximately 20% of the average value, which is an order of magnitude greater than the corresponding values given in Table XII for N_2, O_2, CO, and CO_2. Manual injections reduced this error to within a few percent, so the larger errors were ascribed to nonuniform vaporization of the water under the given conditions. Analysis of water vapor in the reactor off-gas gave peak areas with standard deviations on the same order of magnitude as those obtained with the manual injections.

Table XII. TCD Area Counts and Absolute Response Factors for Water*

Injection No.	Area Counts	Injection No.	Area Counts
1	1,063,416	18	1,424,895
2	1,800,661	19	1,739,656
3	1,465,643	20	1,314,162
4	1,128,829	21	1,873,654
5	1,291,214	22	1,343,012
6	1,219,807	23	1,259,068
7	1,159,253	24	1,617,223
8	1,324,999	25	1,626,117
9	1,949,500	26	1,004,294
10	1,276,468	27	1,468,769
11	1,063,580	28	1,618,706
12	1,013,724	29	1,297,227
13	1,117,679	30	1,358,291
14	1,242,667	31	1,282,054
15	1,039,279	32	1,245,451
16	1,713,941	33	1,057,763
17	1,197,077	34	1,183,742
Average			1,346,524
Standard deviation			258,697
Standard deviation (% of average)			19.21
Absolute response, f (μV-s/μmol)			2,300,891

* The sample loop parameters were a temperature of 473 K, a volume of 500 μL, and a pressure of 1 atm. The calibration liquid was 1.54 mL/h of 10 wt% (4.54 mol%) H_2O in acetone at 21°C.

FID response factors

Table XIII shows the area counts and absolute FID response factors for *n*-butane that were derived from the same set of experiments described above used to determine the TCD response factor. The standard deviation of the area counts from the FID is within 1% of the average area count, which is similar to the result for the TCD response factor as shown in Table X.

Table XIV is similar to Table XIII except that it shows the data used to determine FID response factors for maleic anhydride and tetrahydrofuran, respectively. The experimental protocol was identical to the one used to generate the water calibration data in Table XII, except the solution contained 4.0 wt% maleic anhydride and 4.02 wt% tetrahydrofuran in acetone. The standard deviation for the maleic anhydride area count was within approximately 7% of the average area count, while the standard deviation for tetrahydrofuran was 38.5% of the average

area count. The magnitude of these errors was reduced by an order of magnitude when the sample was introduced with manual injection.

The above methods for determining absolute values for the FID response factors suggested that the magnitude of the standard deviation in the raw area count was on the order of 1% when the calibration mixture was either manually injected or normally exists as a gas and was injected by sampling the flowing calibration standard with the on-line sampling valve. The absolute response factor will have at least this same degree of error, since errors that occur during preparation of the standard and the GC analysis will also contribute to the total error.

When the calibration standard was introduced by pumping a liquid stream and vaporized with a special-purpose in-line device, the standard deviation of the raw area count increased about an order of magnitude, with typical values ranging between 7 and 20% of the average area. The error was likely due to small fluctuations in the liquid volumetric flow rate that resulted in nonuniform vaporization of the liquid mixture. This was supported by the observation that the errors for water were greater than those for either maleic anhydride and tetrahydrofuran. Both the high surface tension and high heat of vaporization of water, when compared with the liquid organic mixture, resulted in poorer wettability of the heated metal surfaces and less uniform vaporization.

Effective carbon numbers

An overall inspection of the chromatograms given in Figures 4–10 shows that the peak shape, resolution, and retention time for a given component can be quite different. This was particularly true for the various WCOT columns that were evaluated for resolution of the oxygenate standard, especially if the comparisons were made between the nonpolar DB-1 column and the polar DB-FFAP column. These qualitative observations of the differences between column performance by comparison of species peak shapes and retention times were useful for providing an initial method for selection of the preferred stationary phase and column attributes, such as column diameter, length, and film thickness. However, a more rigorous assessment of column performance was required, and quantitative analysis and interpretation of the observed responses for each component of interest should be considered. Although various approaches to perform this assessment can be utilized, a particularly useful one relies on quantitative interpretation of the component responses using the effective carbon number (ECN) concept. This method was used to evaluate the performance of the various columns that were tested as part of a more systematic approach for ranking column performance.

The ECN concept provided a quantitative basis for evaluating the expected FID response factor by addition of the group contribution values for different functional groups that were present in a given component. The resulting theoretical values for the ECN of a given component could be compared with experimental ECN values that were derived from chromatographic analysis of standard test mixtures by using a particular column and associated test conditions. Any significant differences between the experimental and theoretical ECN values suggested that several possible effects may be present. These effects include the following: (*a*) the purity of the component used in the standard solution was different than the assumed value used to determine the species composition, (*b*) adsorption on the packing or in the stationary phase was not linear and reversible, or (*c*) some combination of these two effects. Since the purity of the components used to prepare the hydrocarbon and oxygenate standards given in Table V was known, any significant differences between the theoretical and experimental values for the ECN can be ascribed to nonideal interactions between the component of interest and the column packing or stationary phases. Those packings or stationary phases that gave experimental ECN values that were within statistically valid limits of the theoretical values would represent the preferred choice. This assumes that the component was baseline resolved so that errors introduced from integration of nonideal peaks can be considered negligible.

An excellent introduction and overview of the ECN concept with applications is provided by Scanlon and Willis (40) and the references provided therein. Included also in this reference is a list of the recommended group contribution values that can be used to estimate the ECN of a given component. The values for the ECNs of the various components in the hydrocarbon and oxygenate standards were derived using the group contribution values in this latter reference.

It is important to note that some uncertainty exists, however, with respect to the ECNs for furan and furan derivatives, since

Table XIII. FID Area Counts and Absolute Response Factors for *n*-Butane in Nitrogen*

Injection No.	FID Area Counts for *n*-Butane 1%	2%	4%
1	911,614	1,728,161	3,400,543
2	915,510	1,755,616	3,411,312
3	906,616	1,725,337	3,409,264
4	905,591	1,715,393	
5	905,110		
6	910,763		
7	909,201		
Average	909,201	1,731,127	3,407,040
Standard deviation	3753	17,220	5719
Standard deviation (% of average)	0.41	0.99	0.17
Absolute response (μV-s/μmol)	7,053,385	6,714,856	6,607,772
Average response			6,792,004
Standard deviation			232,609

* Note: The sample loop parameters were a temperature of 473 K, a pressure of 1 atm, and a volume of 500 μL. The calibration gas was 1, 2, and 4 mol% of *n*-butane in N_2 (three mixtures). The gas flow rate was 50 sccm at 21°C and 1 atm.

the structures of these compounds are related to those for alcohols and ethers. In a primary alcohol, the ECN is 0.5–0.75 units less than the compound carbon number (40). For this reason, a theoretical ECN of 3.5 was assumed for furan, 2,3-dihydrofuran, and tetrahydrofuran.

The development of the working equation for evaluation of the ECN of a given component relative to an assumed reference component is given by Scanlon and Willis (40). The final expression for the ECN of component *i* is

$$ECN_i = f_{r,i}\, ECN_r \qquad \text{Eq 1}$$

where $f_{r,i}$ is the FID relative response factor for species *i*. This latter quantity is equivalent to the reciprocal of F(R-molar), which is given by Equation 3 in reference 40. It can be expressed in the following equivalent forms, which contain the experimental observables:

$$f_{r,i} = \frac{A_i}{A_r}\frac{n_r}{n_i} = \frac{A_i}{A_r}\frac{w_r}{w_i}\frac{M_i}{M_r} \qquad \text{Eq 2}$$

In Equation 2, *A* denotes the corrected peak area, *n* denotes the molar quantity, *M* is the molecular weight, *w* is the absolute weight, and the subscripts *i* and *r* refer to species *i* and the reference species, respectively. As pointed out by Willis and Scanlon (40), any component in the standard or calibration mixture can be selected as the reference species provided that the effective carbon number is known with a high degree of certainty. Either saturated or unsaturated hydrocarbons are preferred since their ECN is simply equivalent to the number of carbon atoms. For polar mixtures where hydrocarbons may be partially miscible or immiscible, the choice of an oxygenated or other different type of organic species as a reference compound that is soluble at the given composition may be necessary. The results given below for the oxygenate standard were based upon acetone as the primary reference species, since it has a known ECN of 2 and exhibits linear, reversible behavior on the given capillary column stationary phases.

Having described the basis of the ECN concept and the motivation for applying it to the current application, experimental values for the ECNs of selected components in the hydrocarbon and oxygenate standards were obtained and compared with the theoretical values. The experimental values were based on both manual and on-line injections. The composition of these standards is specified in Table V. The raw experimental area response data for each species are given in the supplementary material, which is available directly from the authors on request.

Hydrocarbon standard

The ECNs of selected species in the hydrocarbon standard obtained from the Al_2O_3/PLOT column are given in Table XV. These were based on five repeated injections and were derived by using ethane as the reference component. The percent relative deviations varied between 11% for *n*-butane and –28% for 1,3-butadiene. Most of the experimental values for the ECNs were less than the theoretical values, with the exception of methane and *n*-butane. The standard deviations generally increased with increasing carbon number, with those for methane, propane, propylene, isobutane, and propadiene being less than 0.25. Since the difference between the experimental and theoretical values for the ECNs for most of the compounds were greater than the standard deviations, systematic errors were likely present. The most likely ones were errors in the gas compositions used to derive the experimental ECN values. A detailed study on the errors associated with preparing the gas standards was not conducted, however, since the gas standards were purchased from a commercial source. Repeating the same experiments with another gas blend from the same supplier resulted in both positive and negative percent relative deviations, so gas composition measurements were a likely source of error.

Oxygenate standard

Table XVI shows the ECNs that were derived from four repeated manual injections of the oxygenate standard by using the DB-1 column with a film thickness d_f of 5 µm. The relative deviations for most species were

Table XIV. FID Area Counts and Absolute Response Factors for Maleic Anhydride and Tetrahydrofuran in Acetone Solvent*

Injection No.	FID Area Counts MAN	FID Area Counts THF	Injection No.	FID Area Counts MAN	FID Area Counts THF
1	128,007	452,730	14	129,774	414,377
2	121,559	368,027	15	135,012	253,915
3	137,529	445,864	16	132,457	393,346
4	121,314	684,863	17	137,391	426,381
5	117,506	138,584	18	125,952	383,859
6	115,266	253,992	19	123,131	447,630
7	127,072	403,126	20	130,792	448,712
8	109,005	401,310	21	120,364	284,878
9	124,702	433,054	22	138,059	368,054
10	109,191	395,478	23	120,826	429,693
11	141,947	467,491	24	119,693	428,961
12	112,044	405,550	25	129,118	330,667
13	123,289	412,392	26	127,248	347,565
Average				125,317	393,096
Standard deviation				8804	151,216
Standard deviation (% of average)				7.03	38.47
mol%				0.3448	0.4717
Absolute response, f (µV-s/µ mol)				2,819,560	6,465,032

* The sample loop parameters were a temperature of 473 K, a volume of 500 µL, and a pressure of 1 atm. The calibration liquid was 4 wt% MAN, 4.02 wt% THF, and the balance (91.98 wt%) was acetone at 1.54 mL/h.

generally within ± 20% of the theoretical values, except for 2,3-dihydrofuran. The larger standard deviation was attributed to the high volatility of this component, which introduced larger errors during preparation of the standard mixture. In addition, the ECN results for the combined peak containing isobutyric acid and 2-methoxy tetrahydrofuran were not reported, since their respective ECNs differed and the peak areas of each component were not available.

Inspection of the standard deviations shows that the greatest deviations occured for the C_4 acids and maleic anhydride. The precise reason for these larger deviations has not been determined, but the experimental values for the ECNs were within a standard deviation of the theoretical value. An exception was the value for maleic anhydride. The experimental value of 1.38 for the ECN for maleic anhydride was less than the theoretical value of 2.0 and cannot be explained in terms of experimental errors, since the standard deviation is 0.28. Additional injections with new standards that contained up to 7 wt% maleic anhydride in acetone have consistently yielded a value between approximately 1.35 and 1.45, so the observed value has been used in all subsequent calculations involving quantitation of the raw GC peak area results.

Application to catalyst testing

Development of the multidimensional GC-based method described here was mainly driven by the need to increase the rate of catalyst testing for butane oxidation to maleic anhydride using automated laboratory-scale reactor systems. The literature review suggested that previous chromatographic methods used for hydrocarbon partial oxidation catalyst testing either did not resolve the reaction product gas into all of its substituent components or required various manual techniques for collection of the reactor product gas and subsequent analysis. This method was developed to circumvent these and other related difficulties so that catalyst testing could be performed with a high degree of reliability using unattended, safe operation.

Figure 18 shows the FID and TCD outputs obtained from a typical on-line analysis of a butane oxidation reaction product gas collected from an automated laboratory-scale catalyst testing system was the DuPont Experimental Station with a standard vanadium–phosphorus mixed-metal oxide catalyst. The reactor feed gas for these experiments contained approximately 2% *n*-butane in air. Other experimental particulars are given in the figure caption. The chromatogram corresponding to the FID shows that small amounts of ethane and isobutane were present, which was also observed in feed gas samples. Maleic anhydride, which was the desired oxygenated product, was produced along with minor amounts of methacrolein, tetrahydrofuran, and acrylic acid. Acetic acid, which is also a commonly reported byproduct, was not detected in this particular set of experiments. The chromatogram corresponding to the TCD shows that unreacted O_2 and *n*-butane are present, along with the combustion products associated with *n*-butane, maleic anhydride, and other hydrocarbons. These data, along with the corresponding feed gas analysis and information on the reaction process variables, provide the basis for evaluation of reactant conversions, product selectivities and yields, and other derived quantities that are used to evaluate catalyst performance. These details are omitted here since they are outside the scope of this work, but they are the subject of a future publication.

Summary and Conclusions

A multidimensional gas chromatographic method that resolves and quantitates the C_1–C_4 hydrocarbons, oxygenates, fixed and combustion gases obtained from the gas-phase oxidation of *n*-butane over metal oxide heterogeneous catalysts has been developed and evaluated. Analysis of this reaction mixture provides several unique analytical challenges if all of the components in the mixture must be analyzed to achieve the desired catalyst testing experimental objectives. These challenges occur because the components that comprise the reaction mixture have a wide range of boiling points, some of the species are

Table XV. ECNs for Hydrocarbons with the Al_2O_3/PLOT Column

Compound	Average for all Trials	Theory	SD*	RSD*
Methane	1.06	1.0	0.01	5.89
Ethane	2.00	2.0	0.00	0.00
Propane	2.89	3.0	0.12	- 3.92
Propylene	2.86	3.0	0.12	- 4.90
Iso-Butane	3.71	4.0	0.25	- 7.91
n-Butane	4.49	4.0	0.37	10.98
Allene (propadiene)	2.52	3.0	0.24	-19.02
1-Butene	3.17	4.0	0.49	-26.26
trans-2-Butene	3.26	4.0	0.39	-22.86
Isobutylene	3.30	4.0	0.36	-21.23
cis-2-Butene	3.80	4.0	0.60	- 5.13
1,3-Butadiene	3.12	4.0	0.46	-28.23

Abbreviations: SD, standard deviation; RSD, relative standard deviation.

Table XVI. ECNs for Oxygenates with the DB-1 Column with a Film Thickness of 5 µm

Compound	Average for all Trials	Theory	SD*	RSD*
Acetone	2.00	2.0	0.00	0.00
Furan	3.32	3.9	0.01	5.07
Methacrolein	3.07	3.0	0.04	- 2.42
2,3-Dihydrofuran	1.92	3.5	0.48	45.29
Methyl ethyl ketone	3.88	3.0	0.06	-29.17
Acetic acid	0.80	1.0	0.19	20.50
Tetrahydrofuran	3.50	3.5	0.06	0.14
Crotonaldehyde	2.67	3.0	0.10	11.17
Acrylic acid	1.54	2.0	0.16	22.88
Methacrylic acid	3.27	3.0	0.55	-8.92
Maleic anhydride	1.38	2.0	0.28	30.87
Crotonic acid	2.96	3.0	0.42	1.42

Abbreviations: SD, standard deviation; RSD, relative standard deviation.

thermally unstable and reactive, and the mixture composition can vary widely, depending upon the nature of the catalyst and reaction conditions. The proposed method is robust and is particularly useful for laboratory-scale exploratory research where new catalyst compositions are being evaluated by using an automated reactor facility, since it can resolve and quantitate various byproducts that normally might not occur in a well-seasoned commercial process.

The results of various column evaluations with synthetic mixtures containing representative C_1–C_4 oxygenated products, such as carboxylic acids, aldehydes, ketones, furan derivatives, and maleic anhydride, suggested that either a nonpolar DB-1 wall-coated open tubular (WCOT) megabore column or a slightly polar 1701 WCOT megabore column with two different levels of temperature programming provided good resolution with negligible sample adsorption. Some of the organic acids resulted in slightly unsymmetric peaks on the DB-1 column, but the peak shape improved considerably in later work when a higher rate of temperature programming was identified. Subsequent comparisons between theoretical and experimental values for the FID response factors resulted in good agreement so that irreversible adsorption of the acids on the column could be safely neglected. The peak shape for maleic anhydride was excellent, and the FID response factor relative to *n*-butane was reasonably constant over the required range of concentration.

Megabore columns containing slightly polar stationary phases, such as DB-5, generally resulted in poor resolution of the synthetic oxygenate product mixture. Excellent resolution of all the oxygenates was obtained with a thin film polar DB-FFAP WCOT column with the exception of maleic anhydride, which did not elute because of irreversible adsorption. A porous layer open tubular (PLOT) column containing Al_2O_3/KCl gave excellent resolution of the C_1–C_4 hydrocarbons. Similarly, a packed column containing 23% SP-1700 on 80/100 Chromosorb P AW also gave good resolution of the hydrocarbons, but it was not used since the resolution provided by the Al_2O_3/KCl PLOT column was better. In addition, connection of the megabore DB-1 column and the 23% SP-1700 column in the required series-bypass mode would have required hardware modifications to achieve the needed carrier gas flow rate in the latter column.

It was shown that resolution of O_2, N_2, CO, CO_2, *n*-butane, and water could be performed by using a series-parallel arrangement of ⅛-in. o.d. packed columns containing molecular sieve 5A and Hayesep R on the TCD side. This was possible since the CO, O_2, and N_2 were relatively unretained on the polar Hayesep R column, and they could be adequately resolved on the molecular sieve column. All of the remaining components were reversibly retained on the Hayesep R column and eluted under temperature programmed conditions. Proper selection of the molecular sieve column length allowed the N_2 peak to be sufficiently broadened so that the peak maximum remained on scale without significant broadening of the early eluting CO peak.

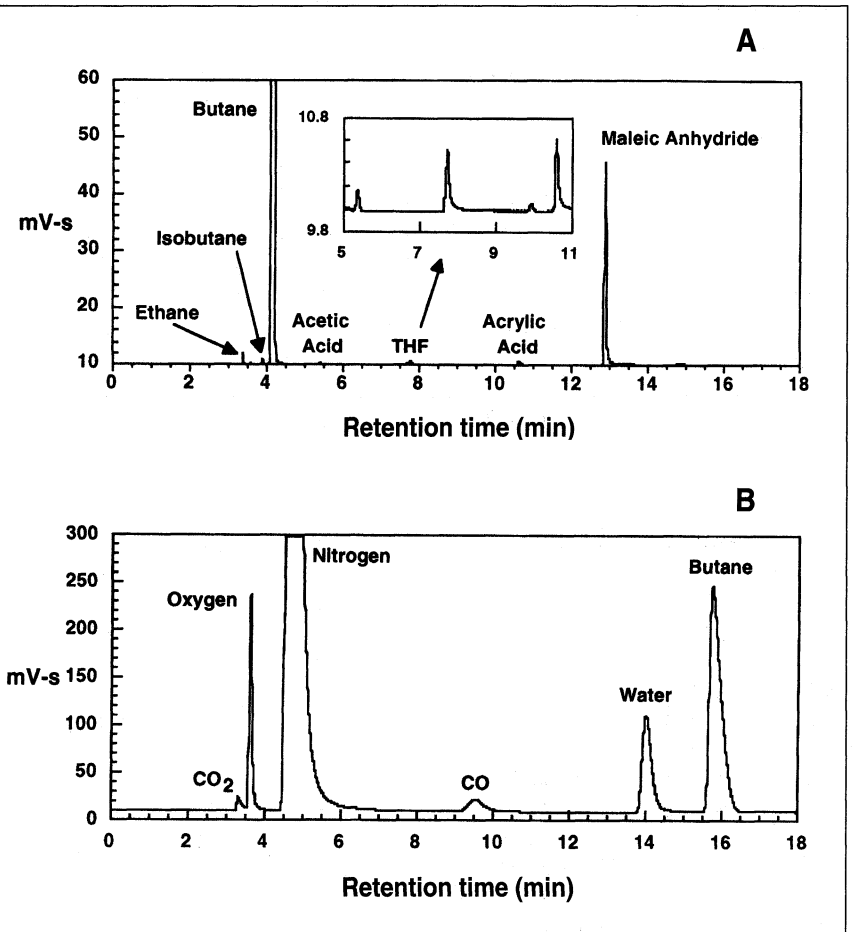

Figure 18. Typical FID and TCD analysis obtained when the method is used in an automated reactor system for screening of a VPO butane oxidation catalyst. Reaction conditions: T = 380°C, Contact time, 3 s.

Since water had been shown in several previous literature studies to have an important effect on the reaction kinetics for *n*-butane oxidation under typical fixed-bed reaction conditions (12,33,39), the quantitation of this species was viewed as a necessary analytical requirement. A number of other TCD-based methods have been described in the literature for resolution of the above mixture in the absence of water, but these were shown to be unsatisfactory in the early stage of method development. A detailed comparison of various columns containing Hayesep porous polymers and other packings proved that Hayesep R gave a water peak with minimal tailing. By selection of the proper column length, it was shown that this packing resolved CO_2 and *n*-butane without overlapping with O_2, N_2, and CO that were simultaneously eluting to the TCD from the molecular sieve column.

Quantitation of the various species with experimentally-based absolute and relative response factors developed from gas and liquid standards resulted in some useful insight on the performance of the detectors and columns over an extended period of operation with a variety of sample compositions. Comparison between experimental and theoretical values of the FID response factors for the

hydrocarbons and oxygenates using the effective carbon number concept (40) suggests that those derived from theoretical values were quite reliable for nearly all species of interest. Maleic anhydride was an anomaly in this respect, since the relative response factor obtained by using *n*-butane as a reference species was about 25% less than the predicted value of 2.

An important feature of the proposed technique was that resolution and quantitation of nearly all primary and secondary *n*-butane reaction products can be achieved in a single, temperature-programmed gas-chromatographic instrument equipped with flame-ionization and thermal conductivity detectors. A critical element of this system was the hardware and protocol associated with sampling the hot reactor feed or product gas stream. This included a heated gas sampling system equipped with multiport valves, sample transfer lines with a deactivated liner for inertness, and a timed sequence of valve actions that were controlled by the automation system. By contrast, previous GC and other analytical methods either did not resolve all of the species present in the product gas matrix or required the use of manual sample collection via product gas condensation with subsequent off-line analysis. The latter approach was required due to complications associated with the capture and transport of a vapor stream containing maleic anhydride, which represented a notoriously difficult sampling problem. Hence, the current approach allowed the operation of a multiple reactor system to be notably simplified since sample collection can be performed on-line and all of the components were resolved. In addition, the effort required to calibrate, operate, and maintain several GC systems that might normally be required with a multiple reactor system was reduced, since only a single instrument would be used. The temperature program for the proposed technique results in a total analysis time of 15 min so that four reaction product samples can be resolved and quantitated every hour.

Use of the method off-line by manual injection with either a gas-tight or liquid syringe was particularly useful for preliminary identification of suspected products by comparison of retention times and for development of relative response factors. Determination of response factors would only be reliable for cases where the components of interest were present in a solvent at a known composition, and an internal standard was also present. Trapping of maleic anhydride and other species that normally exist as either liquid or solids under normal conditions in the reactor off-gas with subsequent manual injection could represent another use of the method in case on-line sampling was not feasible, for example, in certain commercial applications.

Experience in using the proposed method in automated reactor systems over several years of operation with more than fifty thousand injections has shown that it is extremely reliable. The original capillary columns used for the method development continue to provide stable retention times, which is indicative of negligible column degradation. An early concern included the possible degradation of the packed column TCD method due to a lack of a guard column for removal of the heavier boiling components from the gas sample. Stable retention times for O_2, N_2, CO, CO_2, *n*-butane, and water over months of operation and several thousand on-line injections suggest that this effect has been negligible.

Incorporation of the method into other laboratory reactor systems where butane oxidation and other related hydrocarbon oxidations are being studied represents the most likely application in the near future. Use of the method as the basis for development of a process analyzer in a pilot-plant or commercial setting is also quite feasible provided that the sampling system does not alter the composition of the process stream.

Acknowledgments

The authors wish to acknowledge helpful discussions with Dr. Constantin (Gus) Milionis and Dr. Raymond Buchta during the early stages of the method development. Rosalie M. Zubyk, Corporate Analytical, directed the work on the GC–MS analysis of the oxygenate standard with the various capillary columns. Results are given in the supplementary material. Dr. John Sullivan of the CR&D Catalysis Center contributed the results shown in Figure 18. J. Scott McCracken and Thomas M. Delaney provided valuable assistance during preparation of the revised manuscript. Finally, we acknowledge the suggestions of Dr. Donald E. Willis on proper application and use of the ECN concept.

References

1. W.D. Robinson and R.A. Mount. Maleic anhydride, maleic acid, and fumaric acid. In *Kirk-Othmer Encyclopedia of Chemical Technology*, 3rd ed. H.F. Mark, D.F. Othmer, C.G. Overberger, and G.T. Seaborg, Eds. Wiley, New York, NY, 1981, pp 770–93.
2. B.C. Privedi and R.M. Culbertson. Maleic Anhydride. Plenum Press, New York, NY, 1982.
3. R.M. Culbertson. Maleic and fumaric polymers. In *Encyclopedia of Polymer Science and Engineering*. H.F. Mark, N.M. Bikales, C.G. Overberger, and G. Menges, Eds. Wiley, New York, NY, 1987, pp 225–94.
4. S.D. Cooley and J.D. Powers. Maleic acid and anhydride. In *Encyclopedia of Chemical Processing and Design*. J.J. McKetta and W.A. Cunningham, Eds. Marcel-Dekker, New York, NY, 1988, pp 35–55.
5. K. Lohbeck, H. Hafferkorn, W. Fuhrmann, and N. Fedtke. Maleic and fumaric acids. In *Ullman's Encyclopedia of Industrial Chemistry*, 5th ed. B. Elvers, S. Hawkins, and G. Schulz, Eds. VCH Press, Weinheim, Germany, 1990, pp 53–62.
6. K. Wessermel and H.J. Arge. *Industrial Organic Chemistry*, 2nd ed. VCH Press, Weinheim, Germany, 1990, pp 362–69.
7. D.A. De Maio. Will butane replace benzene as a feedstock for maleic anhydride? *Chem. Eng.* May 19, 1980.
8. F. Cavani and F. Trifiro. Some innovative aspects in the production of monomers via catalyzed oxidation processes. *Appl. Catal. A: General* **88:** 115–35 (1992).
9. A Practical Guide to Catalyst Testing. J.C. Schlattler, Ed. Catalytica Study No. 4186 TE, Catalytica, Mountain View, California, 1987.
10. E.G. Christoffel. Laboratory studies of heterogeneous catalytic processes. *Studies in Surface Science and Catalysis*. B. Delmon and J. T. Yates, Eds. Elsevier, Amsterdam, 1989, pp 185–254.
11. P.L. Mills and J.J. Lerou. Laboratory reactors for transient studies of gas-phase heterogeneous catalyzed reactions. Experimental techniques and mathematical modeling. *Rev. Chem. Eng.* **9:** 1–96 (1993).
12. J.J. Lerou and P.L. Mills. DuPont butane oxidation process. In *Precision Process Technology*. M.P.C. Weijnen and

A.A.H. Drinkenburg, Eds. Kluwer Academic, Amsterdam, The Netherlands, 1993, pp 175–95.
13. G. Centi, Ed. Forum on Vanadyl Pyrophosphate Catalyst. *Catal. Today* **16** (1993).
14. M. Akimoto and E. Echigoya. Hydrocarbon species selective to maleic anhydride formation in vapor-phase oxidation of butadiene over supported molybdena catalyst. *J. Catal.* **31:** 278–86 (1973).
15. M. Akimoto and E. Echigoya. Competition of the two reaction mechanisms of maleic anhydride formation in vapor-phase oxidation of butadiene over supported molybdena catalyst. *Bull. Chem. Soc. Jpn.* **48:** 3518–22 (1975).
16. M. Ai. The activity of WO3-based mixed-oxide catalysts II. Activity and selectivity in oxidations of butene and butadiene. *J. Catal.* **49:** 313–19 (1977).
17. A.I. Pyatnitskaya, G.A. Kamasho, V.A. Zazhigalov, and Y.B. Gorokhovatskii. *n*-Butane oxidation over a vanadium–phosphorus catalyst. *React. Kinet. Catal. Lett.* **6:** 341–48 (1977).
18. E. Bordes and P. Courtine. Some selectivity criteria in mild oxidation cataysis. V-P-O phases in butene oxidation to maleic anhydride. *J. Catal.* **57:** 236–52 (1979).
19. D. Vanhove, S.R. Op, A. Fernandez, and M. Blanchard. Catalytic oxidation of 1-butene and butadiene. Study of MoO_3-TiO_2 catalysts. *J. Catal.* **57:** 253–63 (1979).
20. D. Vanhove, A. Fernandez and M. Blanchard. On the occurrence of competitive mechanisms in the transformation of butadiene into maleic anhydride with air on MoO_3-TiO_2 catalysts. *React. Kinet. Catal. Lett.* **14:** 467–73 (1980).
21. M. Ai. The production of furan by the vapor-phase oxidation of butadiene using heteropoly compounds as catalysts. *J. Catal.* **67**: 110–17 (1981).
22. H. Miura, Y. Arai, K. Sugiyama, and T. Matsuda. Mechanism of 1-butene oxidation in connection with the layer structure of Bi_2MoO_6 catalyst. *J. Catal.* **68**: 264–69 (1981).
23. G. Franz, F. Nierlich, and H.J. Ratajczak. Maleic anhydride production from C_4 hydrocarbons by oxidation over catalyst containing tungsten, molybdenum, and antimony. U.S. Patent 4, 208, 448 assigned to Chem. Werke Huls AG, 1981.
24. L. Morselli, F. Trifiro, and L. Urban. Study of the interaction of 1-butene with V2O5 and mixed vanadium and phosphorus oxides by means of temperature programmed desorption. *J. Catal.* **75:** 112–21 (1982).
25. G. Centi, G. Fornasari, and F. Trifiro. On the mechanism of *n*-butane oxidation to maleic anhydride: Oxidation in oxygen stoichiometry-controlled conditions. *J. Catal.* **89:** 44–51 (1984).
26. J.T. Gleaves, J.R. Ebner, and T.C. Kuechler. Temporal analysis of products (TAP)—A unique catalyst evaluation system with submillisecond time resolution. *Catal. Rev. Sci. Eng.* **30:** 49–116 (1988).
27. G. Centi, F. Trifiro, J.R. Ebner, and V.M. Franchetti. Mechanistic aspects of maleic anhydride synthesis from C_4 hydrocarbons over phosphorus-vanadium oxide. *Chem. Rev.* **88:** 55–80 (1988).
28. G J. Hutchings. Effect of promoters and reactant concentration on the selective oxidation of *n*-butane to maleic anhydride using vanadium-phosphorus oxide catalysts. *Appl. Catal.* **72:** 1–32 (1991).
29. S.K. Bej and M. Rao. Selective oxidation of *n*-butane to maleic anhydride. *Appl. Catal.* **83:** 149–63 (1992).
30. G. Emig and F.G. Martin. Development of a fluidized-bed catalyst for the oxidation of *n*-butane to maleic anhydride. *Ind. Eng. Chem. Res.* **30:** 1110–16 (1991).
31. M.A. Pepera, J.L. Callahan, M.J. Desmond, E.C. Milberger, P.R. Blum, and N.J. Bremer. Fundamental study of the oxidation of butane over vanadyl pyrophosphate. *J. Am. Chem. Soc.* **107:** 4883–92 (1985).
32. F. Cavini, G. Centi, and F. Trifiro. Study of *n*-butane oxidation to maleic anhydride in a tubular flow stacked-pellet reactor. Influence of phosphorus on selectivity. *Appl. Catal.* **15:** 151–60 (1985).
33. J.S. Buchanan and S. Sundaresan. Kinetics and redox properties of vanadium phosphate catalysts for butane oxidation. *Appl. Catal.* **26:** 211–26 (1986).
34. R K. Sharma, D.L. Cresswell, and E.J. Newson. Kinetics and fixed-bed reactor modeling of butane oxidation to maleic anhydride. *AIChE J.* **37:** 39–47 (1991).
35. S.K. Bej and M.S. Rao. Selective oxidation of *n*-butane to maleic anhydride. 1. Optimization Studies. *Ind. Eng. Chem. Res.* **30:** 1819–24 (1991).
36. S.K. Bej and M.S. Rao. Selective oxidation of *n*-butane to maleic anhydride. 2. Identification of the rate expression for the reaction. *Ind. Eng. Chem. Res.* **30:** 1824–28 (1991).
37. S.K. Bej and M.S. Rao. Selective oxidation of *n*-butane to maleic anhydride. 3. Modeling studies. *Ind. Eng. Chem. Res.* **30:** 1829–32 (1991).
38. S K. Bej and M.S. Rao. Selective oxidation of *n*-butane to maleic anhydride. 4. Recycle reactor studies. *Ind. Eng. Chem. Res.* **31:** 2075–79 (1992).
39. J.J. Lerou. Butane oxidation kinetics. 25th Annual Spring Symposium of the Pittsburgh-Cleveland Catalysis Society, Cleveland, Ohio, May 1986.
40. J.T. Scanlon and D.E. Willis. Calculation of flame ionization detector relative response factors using the effective carbon number concept. *J. Chromatogr. Sci.* **23:** 333–40 (1985).
41. R. Boulet, J. Buzøn, and J.C. Roussel. Coupling of gas chromatography and mass spectrometry. *Ind. Chim. Belge* **32:** 227–31 (1967).
42. A. Di Lorenzo. Quantitative analysis of maleic and citraconic anhydrides by gas chromatography. *J. Chromatogr.* **55:** 303–308 (1971).
43. L.I. Mariich and I.A. Zelenskaya. Impurities and control of phthalic anhydride quality studied by a gas-liquid chromatographic method. *Khim. Tekhnol (Kiev)* **6:** 60–62 (1971).
44. L I. Mariich, I.A. Zelenskaya, and V. I. Filippov. Chromatographic monitoring of the production and quality of phthalic anhydride. *Sb. Nauch. Trr., Ukr. Nauch. -Issled. Uglekhim Inst.* **24:** 142–48 (1971).
45. J. Guberska, B. Draniak, and A. Dzostak. Possibilities of using gas chromatography for the determination of *o*-xylene and naphthalene oxidation products. *Chem. Anal. (Warsaw)* **21:** 1161–69 (1976).
46. H. Ide and H. Arimitsu. Analytical method for phthalic acid anhydride. *Aromatikkusu* **30:** 436–42 (1978).
47. A.A. Lyapkin and L.M. Smirnykh. Gas-chromatographic analysis of products of a phthalo-air mixture. *Khim. Prom-st. Ser.* **7:** 3–5 (1980).
48. A.S. Trynkina and N.B. Shepot'ko. Gas-chromatographic analysis of a phthalo-air mixture. *Khim. Prom-st., Ser.* **11:** 8–10 (1981).
49. V.I. Zheivot, M.E. Shalaeva, V.Y. Gavrilov, V.B. Fenelonov, I.A. Ovsyannikova, and V.V. Malakhov. Intermolecular interactions in the sorbate-modified graphitized thermal carbon black system. *J. Chromatogr.* **472:** 155–61 (1989).
50. A.A. Shapovalov, I.I. Kan, N.I. Chukhno, D.K. Sembaev, and B.V. Suvorov. Analysis of products of the oxidation and oxidative ammonolysis of *o*-xylene, naphthalene, and their *tert*-butyl derivatives by a gas–liquid chromatographic method. *Izv. Akad. Nauk Kaz. SSR, Ser. Khim.* **2:** 49–52 (1979).
51. G.D. Mitra and S.K. Ghosh. Analysis of toluene oxidation products by programmed temperature gas chromatography. *Fert. Technol.* **17:** 194–96 (1980).
52. M. Balakova and A. Vanko. Contribution to problems of quantitative analysis using gas-liquid chromatography. *Petrochemia* **17:** 26–36 (1977).
53. Authors Unknown, Analytical monitoring of the hydrogenation of maleic anhydride in γ-butyrolactone and tetrahydrofuran. *Zh. Prikl. Khim. (Leningrad)* **51:** 896–900 (1978).
54. W. Fiebig, H. Ewald, and G. Oehlmann. Qualitative and quantitative gas chromatographic detection of maleic acid in the presence of C_2–C_4 monocarboxylic acids. *Chem. Tech. (Leipzig)* **32:** 40–42 (1980).
55. I. Hopartean, N. Dulamita, and M. Vagaonescu. Gas chromatographic determination of the products obtained by catalytic reduction of maleic anhydride. *Stud. Univ. Babes-Bolyai Chem* **31:** 63–67 (1986).

56. S.D. Bhagat. Gas-chromatographic method to monitor the synthesis of *N*-methyl-2-pyrrolidone. *Ind. J. Technol.* **28:** 71–74 (1990).
57. R.H. Brown and C.J. Purnell. Collection and analysis of trace organic vapor pollutants in ambient atmospheres. The performance of a Tenax-GC adsorbent tube. *J. Chromatogr.* **178:** 79–90 (1979).
58. K. Ventura and R. Matuska. Determination of maleic anhydride in workplace air. *Chem. Prum.* **40:** 546–48 (1990).
59. P.A. Poppisil, M.F. Marcus, and M.A. Kobus. The application of supercritical fluid capillary chromatography to the analysis of Appendix-VIII and IX compounds. ASTM Spec. Tech. Publ., STP 1075 (Waste Test Qual. Assur., 3rd Vol), 154–69 (1992).
60. A.I. Lamotkin and A.N. Pronevich. Determination of maleic anhydride in terpene-maleic resins and in wastewater from their manufacture. *Gidroliz. Lesokhim. Prom-st.* **2:** 6–7 (1991).
61. H. Zowall. Use of a pyrolytic attachment for detection of small amounts of propylene oxide, epichlorohydrin, and maleic anhydride in polyester resins by gas chromatography. *Polimery (Warsaw)* **23:** 133 (1978).
62. V.A. Zazhigalov and Y.P. Zaitsev. Effect of steam on the catalytic oxidation of butane and formation of maleic anhydride. *Kinet. Katal.* **20:** 54–56 (1982).
63. B. Müller and M. Baerns. Direct gas chromatographic determination of the products of catalytic air oxidation of n-butene-1 to maleic anhydride in the gaseous mixture. *J. Chromatogr.* **214:** 2217–21 (1981).
64. P. Centola, R. Del Rosso, G. Terzaghi, C. Mazzocchia, and E. Albertario. Gas-chromatographic analysis of effluents from a butene oxidation reactor. *Chim. Ind. (Milan)* **54:** 703–705 (1972).
65. Y.P. Zaitsev and V.A. Zazhigalov. Use of mathematical methods of experimental design in selecting optimum parameters of the separation of C_2–C_4 hydrocarbon oxidation products by a gas-chromatographic method. In *Tezisy Dokl. - Twelfth Ukr. Resp. Konf. Fiz. Khim.* K.B. Yatsimirskii, Ed. Izd. Naukova Dumkra, Kiev, USSR, 1977, pp 175–76.
66. Y.P. Zaitsev and V.A. Zazhigalov. Use of mathematical methods of experimental design in the selection of optimum parameters for the separation of C_2–C_4 hydrocarbon oxidation products by a gas-chromatographic method. *Katal. Katal.* **18:** 94–97 (1980).
67. C. Laguerie and M. Aubry. Catalytic oxidation of butane. Gas chromatographic separation and analysis of the reaction products. *J. Chromatogr.* **101:** 357–64 (1974).
68. A. Aguero, R.P.A. Sneeden, and J.C. Volta. Selective-oxidation on vanadyl phosphate catalysts: Oxidation of linear and branched alkanes. *In Hetergeneous Catalysts and Fine Chemicals: Studies on Surface Science and Catalysis.* Vol XX. M. Guisnet, Ed. Elsevier, Amsterdam, The Netherlands, 1988, pp 353–59.
69. M.S. Wainwright and T.W. Hoffman. Gas chromatographic analysis of *o*-xylene oxidation products. *J. Chromatogr. Sci.* **14:** 159–62 (1976).
70. N.R. Foster and M.S. Wainwright. On-line gas chromatographic analyses for phthalic anhydride manufacture. *Chromatographia* **11:** 19–22 (1978).
71. O. Kiser, T.Q. Phung-Quach, D. Klvana, and B. Gilot. Chromatographic analysis of the products of catalytic oxidation of benzene. *J. Chromatogr.* **151:** 81–86 (1978).
72. S. Lars and T. Andersson. Gas chromatographic analysis of toluene oxidation products. *J. Chromatogr. Sci.* **23:** 17–21 (1985).
73. N. Vonk, J. de Zeeuw, M. Monhke, and J. Buyten. New selective PLOT columns for the separation of hydrocarbon and volatile organic compounds in the range of C_1–C_6. Paper presented at the International Symposium on Capillary Column Chromatography, May 1992.
74. W.A. Dietz. Response factors for gas chromatographic analyses. *J. Gas Chromatogr.* **5:** 68–71 (1967).

Manuscript accepted February 26, 1996.